

Towards Realistic Minimum-Cost Optimization of Viscous Fluid Dampers for Seismic Retrofitting

Nicolò Pollini^{*1}, Oren Lavan^{†1} and Oded Amir^{‡1}

¹Faculty of Civil and Environmental Engineering, Technion - Israel Institute of Technology, Haifa, Israel

This is an unformatted version of the paper, published online in *Bulletin of Earthquake Engineering*, November 2015. [[http](#)]

Abstract

This paper presents an effective approach for achieving minimum cost designs for seismic retrofitting using viscous fluid dampers. A new and realistic retrofitting cost function is formulated and minimized subject to constraints on inter-story drifts at the peripheries of frame structures. The components of the new cost function are related to both the topology and to the sizes of the dampers. This constitutes an important step forward towards a realistic definition of the optimal retrofitting problem. The optimization problem is first posed and solved as a mixed-integer problem. To improve the efficiency of the solution scheme, the problem is then re-formulated and solved by nonlinear programming using only continuous variables. Material interpolation techniques, that have been successfully applied in topology optimization and in multi-material optimization, play a key role in achieving practical final design solutions with a reasonable computational effort. Promising results attained for 3-D irregular frames are presented and compared with those achieved using genetic algorithms.

Keywords: Topology optimization; Energy dissipation devices; Viscous dampers; Seismic retrofitting; Material interpolation functions; Irregular structures.

1 Introduction

Earthquakes are catastrophic events that pose a threat to infrastructure, to economic systems and to human lives. In recent years many researchers focused on delineating the best methods to mitigate the losses caused by earthquakes using innovative means. As a result, various novel concepts for structural protection have been proposed, are currently under development or have matured to the level of use in practice. Modern structural protective systems can be divided into three major groups: 1) Seismic isolation systems; 2) Passive energy dissipation systems; and 3) Active and semi-active systems. In particular, passive energy dissipation devices are known to be effective for mitigating earthquake hazards and hold an advantage of not requiring an external source of power, Constantinou et al. (1998). The purpose of passive devices is to dissipate part of the input energy, thus reducing the energy dissipation demand of structural members and consequently reducing the structural damage. The use of passive energy dissipation devices is gaining much attention in academia and practice, and the reader is referred to the comprehensive textbooks for more details (Soong and Dargush (1997); Takewaki (2011); Christopoulos et al. (2006)).

Among the available passive energy dissipation systems, viscous fluid dampers have been shown to be very effective in reducing various seismic responses. This is particularly true in the case of retrofitting due to the out-of-phase effect that may eliminate the need for strengthening of foundations and columns (Constantinou and Symans (1992); Lavan (2012)). Furthermore, it was shown that the use of such dampers can reduce the sensitivity to uncertainty in structural properties, Avishur and Lavan (2010).

*nicolo@campus.technion.ac.il

†lavan@cv.technion.ac.il

‡odedamir@cv.technion.ac.il

The focus of this paper is on deriving an efficient optimal design approach for minimizing the actual cost associated with retrofitting of frame structures using viscous fluid dampers.

Several authors focused on the seismic retrofitting of 3-D structures using viscous dampers (e.g. Wu et al. (1997); Goel (1998); Takewaki et al. (1999); Goel (2000); Singh and Moreschi (2001); Lin and Chopra (2001); Kim and Bang (2002); Lin and Chopra (2003a); Lin and Chopra (2003b); Lavan and Levy (2006); Levy and Lavan (2006); García et al. (2007); Almazán and de la Llera (2009); Lavan and Levy (2009); Aguirre et al. (2013); Lavan (pted), Bigdeli et al. (tted)). Some of the above mentioned approaches define optimal distributions of dampers, treating the damping coefficients as continuous design variables independent from one another. This makes the optimal design process computationally efficient and applicable also to large scale problems. However, it implies that the optimized design attained may consist of a wide variety of different damper sizes. Hence, in order to translate these solutions into practical damper distributions, some rounding and grouping of the dampers to a limited number of size-groups is required. While this approach may provide reasonable practical designs in some cases, there is no guarantee of that – nor of the optimality of the interpreted design.

Other methodologies make use of discrete variables to represent the damping coefficients thus promoting a small number of size-groups (e.g. Zhang and Soong (1992); Agrawal and Yang (1999); Lopez Garcia and Soong (2002); Dargush and Sant (2005); Lavan and Dargush (2009); Kanno (2013)). Thus, the attained design does not require any rounding or grouping. However, such approaches make use of predetermined parameters for the damping, such as the dampers' sizes, damping increments, the number of dampers or a combination of these. The values adopted for the damping parameters may have a considerable restraining effect on the optimal solution to be attained. Furthermore, in some of the cases mentioned above the resulting optimization problems are relatively difficult to solve, compared to problems with continuous variables – due to the combinatorial nature of the optimization problem. This imposes a certain limit on the number of design variables – representing damper locations and sizes – that can be considered.

Recently, in Lavan and Amir (2014) an optimization formulation that overcomes these limitations was presented. In their approach, viscous fluid dampers with identical properties, taken as continuous variables and determined by the optimization algorithm rather than a-priori, were optimally allocated by the algorithm. The objective function that was minimized was equivalent to the manufacturing cost of the dampers. Constraints were imposed to limit the inter-story drifts of the peripheral frames, based on time-history analyses under a suite of realistic ground motions. The nonlinear optimization problem was solved by a sequential linear programming procedure utilizing first-order information. In other works, two mixed-integer approaches for the optimal sizing and placement of friction dampers were proposed in Miguel et al. (2014) and Miguel et al. (2015). They referred to the context of human-induced vibrations on footbridges, and of structures subject to seismic loading, respectively. Binary variables were considered to describe the existence of a damper, and continuous variables to characterize the friction forces of each damper. In particular, in Miguel et al. (2014) the objective was to minimize the maximum acceleration of the structure using a metaheuristic algorithm presented in Yang (2008) – the Firefly Algorithm. In Miguel et al. (2015) the goal was to minimize the maximum inter-story drift of a shear frame, and the maximum displacement of a transmission tower with the Backtracking Search Optimization Algorithm recently presented in Civicioglu (2013). In both cases, the number of added dampers and the friction forces of each damper were constrained.

In the above mentioned studies on optimal seismic retrofitting with dampers, the objective functions considered only the cost associated with manufacturing of the dampers. In practical retrofitting, in addition to the direct manufacturing cost, two other dominant cost components, that may sometimes be even larger than the manufacturing cost, should be considered: a) The cost of prototype testing and design of a damper which is proportional to the number of different damper sizes used; and b) The costs of interfering with regular activities in the building and of mounting the dampers, both proportional to the number of locations of the frame in which dampers are mounted.

In this paper we present and solve an optimization problem with an objective function that considers these new cost components. Thus, the resulting cost formulation will consider the initial cost due to the retrofitting with viscous fluid dampers. In addition, we allow the allocation of up to two dampers at each potential location, thus enriching the space of possible design configurations. These advancements constitute an important step towards an optimization problem formulation that adequately represents

reality, and that can facilitate the development of computational tools that are useful for practitioners. From a mathematical point of view, these make the optimization problem much more complex to solve. It should be noted that in some recent work the life-cycle cost has been taken as the objective function for similar problems (e.g. Shin and Singh (2014a); Shin and Singh (2014b); Gidaris and Taflanidis (2014)). These approaches considered different cost components, such as the initial cost, the maintenance cost, and the failure cost. While providing comprehensive formulations of the long term costs, they considered relatively simple formulations of the initial cost related to the use of viscous fluid dampers. In our approach we focus on a more thorough description of the initial retrofitting cost, which considers all the main aspects involved and which is still formulated simply enough to serve practitioners in their activity.

In the optimization problem presented in this paper linear viscous fluid dampers from up to two size-groups are optimally distributed in predetermined potential locations of 3D irregular frames. In each size-group, all dampers have identical properties (e.g. damping coefficient, capacity etc.). The damping coefficient of each size-group is a continuous design variable optimally defined in the optimization analysis. Inter-story drifts at the peripheries are constrained to allowable values, while the above mentioned new formulation for the initial retrofitting cost is minimized. Due to their binary nature, the new features of the cost function considerably increase the complexity of the optimization problem. We first formulate the problem using mixed variables. This leads to a mixed-integer formulation that can be solved by metaheuristic algorithms such as genetic algorithms (GA). This was demonstrated in a recent short conference paper by the authors, Pollini et al. (2014). The main contributions of the present work are the re-formulation and the solution of the same optimization problem using only continuous variables, leading to a more effective computational procedure. Material interpolation techniques, typically applied in topology optimization, are used to force some of the variables to discrete values. The new cost function is modified so that it would be continuously differentiable. Finally, the continuous formulation is solved using a gradient-based algorithm, requiring in this way a more reasonable computational effort. The results, in terms of optimized designs and computational performance, are compared favorably to those achieved with the GA.

The remainder of the article is organized as follows. In Section 2 we present the variables and functions involved, with particular attention to the new cost function. This allows us to present the original formulation of the optimization problem, namely the mixed-integer formulation. In Section 3 we present the continuous formulation of the optimization problem as well as various details regarding the gradient-based approach used in the optimization process. In Section 4 the numerical results corresponding to the optimization of realistic irregular frames are presented, including a comparison between the results achieved with the GA and with the gradient-based algorithm. In Section 5 some final considerations and conclusions are drawn.

2 Mixed-integer approach

In this paper we formulate and solve the optimization problem of minimizing a realistic cost of seismic retrofitting using linear viscous fluid dampers. The dampers can be mounted in predetermined potential locations of a frame, while the design is limited to the use of only a few damper sizes which are determined by the algorithm. The minimization is subjected to constraints on envelope peak inter-story drifts of the peripheral frames in a 3D irregular structure excited by a suite of ground motions. The variables adopted to represent the damping coefficient for each size-group of dampers are continuous, while the existence of a damper in a potential location of the frame and its belonging to a particular size-group of dampers are expressed through discrete variables. The current implementation incorporates two possible size-groups of dampers and up to two dampers for each potential location (see the illustrative example in Fig. 1 that will be explained in the next section). However, due to the generality of the proposed approach it can be extended to accommodate additional size-groups of dampers.

The optimization problem is formulated based on the following components:

- The objective function to be minimized, i.e. the cost function;
- Behavioral inequality constraints imposed on inter-story drifts;
- Behavioral equality constraints representing dynamic equilibrium;

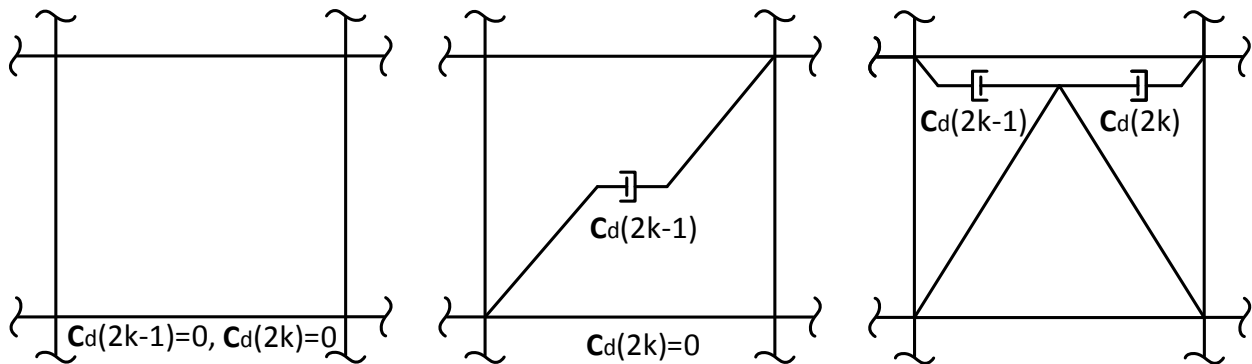


Figure 1: No damper, a single damper, or two dampers in the k^{th} potential location.

- Upper and lower limits on the design variables.

2.1 Design variables and functions definitions

In this section, several variables that play an important role in the proposed formulation are introduced. In the proposed formulation, N_d potential locations for the dampers are defined a-priori by the user. Each potential location is a "cell" of the frame, that is, one bay of one story of a given frame. In each of these locations, up to two dampers could be assigned. We will refer to these dampers hereafter as "the first damper" and "the second damper". Measures will be taken such that assigning the first damper to a given location will be more expensive than assigning the second damper. In addition, assigning the second damper will be prevented if the first damper is not assigned at that location. The damping coefficients of all dampers (first and second dampers in each potential location) are defined in the vector \mathbf{c}_d as follows:

$$\mathbf{c}_d = \bar{c}_d \mathbf{x}_1 (y_1 + (y_2 - y_1) \mathbf{x}_2), \quad (1)$$

where y_1 and y_2 are continuous design variables that scale the maximum damping coefficient, \bar{c}_d , to result in the damping coefficients of the first and second size-groups, respectively. Thus, the two size-groups of dampers are characterized by the following two damping coefficients:

$$\bar{c}_1 = y_1 \bar{c}_d, \quad \bar{c}_2 = y_2 \bar{c}_d. \quad (2)$$

\mathbf{x}_1 and \mathbf{x}_2 are vectors of binary variables. A value of one at a given entry of \mathbf{x}_1 indicates the assignment of the corresponding damper while a value of zero indicates that the damper is not assigned. A value of zero at a given entry of \mathbf{x}_2 indicates that, if the damper is indeed assigned, it belongs to the first size-group, while a value of one indicates that it belongs to the second size-group. Note that the dimensions of the vectors \mathbf{c}_d , \mathbf{x}_1 and \mathbf{x}_2 are $2N_d \times 1$. The entry $2k - 1$ of these vectors corresponds to the first damper at the location k while the entry $2k$ corresponds to the second damper at that location (Fig. 1). Consequently, the damping coefficient added to the location k is:

$$\mathbf{c}_{d_{TOT}}(k) = \mathbf{c}_d(2k - 1) + \mathbf{c}_d(2k). \quad (3)$$

Note that the size of the vector $\mathbf{c}_{d_{TOT}}$ is $N_d \times 1$. Through a proper matrix transformation, which depends on the geometry of the structure, the vector $\mathbf{c}_{d_{TOT}}$ defines the added damping matrix \mathbf{C}_d (Lavan and Levy (2006)).

2.2 Objective function

One of the main aims of the present work is to propose an optimization approach for minimizing a realistic formulation of the retrofitting cost due to the added damping in a structure. This cost function, which is the objective function in the optimization problem, is composed of three components: $J = J_l + J_m + J_p$.

The first component J_l represents the cost associated with the number of locations in which dampers are installed. This cost entails all the aspects of preparing the structure for the damper installation and the architectural constraint that this installation will represent. Moreover, in case of retrofitting, the removal of existing nonstructural components is also considered. We allow the algorithm to allocate as many as two dampers in each potential location, and it will be more expensive to allocate the first damper in an empty potential location than to allocate the second damper in a location where a damper already exists. The first component of the cost is defined as follows:

$$J_l = \mathbf{x}_1^T \mathbf{C}_{mont}, \quad (4)$$

where \mathbf{C}_{mont} is a $2N_d \times 1$ vector in which the i^{th} component is a cost component related to the i^{th} component of \mathbf{x}_1 . The vector \mathbf{C}_{mont} is defined as follows:

$$\mathbf{C}_{mont} = D(\mathbf{C}_{m1}) \begin{bmatrix} 1 \\ 0 \\ 1 \\ 0 \\ \vdots \end{bmatrix} + D(\mathbf{C}_{m2}) \begin{bmatrix} 0 \\ 1 + (1.5 + \frac{\mathbf{C}_{m1}(1)}{\mathbf{C}_{m2}(2)})(1 - \mathbf{x}_1(1)) \\ 0 \\ 1 + (1.5 + \frac{\mathbf{C}_{m1}(3)}{\mathbf{C}_{m2}(4)})(1 - \mathbf{x}_1(3)) \\ \vdots \end{bmatrix}, \quad (5)$$

where D is a matrix operator that transforms a vector into a diagonal matrix (similar to the "diag" function in MATLAB); \mathbf{C}_{m1} represents the specific cost of installation of the first damper in a potential location, its dimensions are $2N_d \times 1$ and it has N_d elements different from zero; \mathbf{C}_{m2} represents the cost for each potential location of adding the second damper assuming the first damper is already installed at that location, its dimensions are $2N_d \times 1$ and it has N_d elements different from zero. Both \mathbf{C}_{m1} and \mathbf{C}_{m2} are vectors defined by the user. Because $\mathbf{C}_{m1}(2k - 1) \geq \mathbf{C}_{m2}(2k) \forall k$, the cost of installing the first damper in a potential location is larger than the cost of installing the second one, provided the first damper is non-zero. The vector that multiplies $D(\mathbf{C}_{m2})$ is defined so that it will be more expensive to first allocate the second damper in an empty location than to allocate the first one in the same location: Referring to the i^{th} location, in the first case the cost will be $\mathbf{C}_{m1}(2i - 1) + 2.5 \times \mathbf{C}_{m2}(2i)$ while in the second case only $\mathbf{C}_{m1}(2i - 1)$.

In formulating J_m , we presume that the cost of a single fluid viscous damper is a function of the peak force it is designed for and of its stroke (maximum elongation). In practice, dampers of the same size-group are designed to have the same properties, hence a size-group of dampers is designed to take the peak stroke expected in the most elongated damper of the same size-group. The peak stroke is strongly correlated with the peak inter-story drift, which is constrained in our problem formulation. For this reason damper stroke is not considered in the cost formulation. Each size-group of dampers is also designed for the peak force of the most loaded damper of that size-group. Therefore, this peak force should be considered in the cost. Assuming a dominant mode behavior, the velocity in the damper in location j is proportional to $\omega_1 d_j$, where ω_1 is the dominant frequency and d_j is the envelope peak drift at the location j . Experience shows that usually dampers are located where the drifts reach their allowable values, that are known values. Thus the maximum velocities are known in advance and minimizing the damping coefficient is equivalent to minimizing the peak force of the most loaded damper of a particular size-group. The number of dampers of each size-group also has a considerable effect on the cost. Thus the component J_m of the cost should mimic the maximum envelope peak force in the damper of any given size-group, multiplied by the number of dampers of that size-group. It should be noted that the cost for a single damper somewhat reduces if more dampers of its size-group are purchased Taylor (2014). However, normally this does not have a significant effect on the optimal solution. Based on the considerations above, the J_m component is defined as follows:

$$J_m = \bar{c}_d \mathbf{x}_1^T (y_1 \mathbf{1} + (y_2 - y_1) \mathbf{x}_2), \quad (6)$$

where the vector $\mathbf{1}$ is a unit vector of size $2N_d \times 1$.

The third component of the cost J_p reflects the cost associated with the requirements of modern seismic codes. These require that a prototype of each size-group of dampers is tested so as to verify

its force-velocity behavior. Therefore, the number of different damper size-groups should be minimized. This can be defined as follows:

$$J_p = C_{prototype} [\mathcal{H}(\mathbf{x}_1^T \mathbf{x}_2) + \mathcal{H}(\mathbf{x}_1^T (\mathbf{1} - \mathbf{x}_2))], \quad (7)$$

where $C_{prototype}$ is the cost of prototype testing and design. The function \mathcal{H} is the Heaviside step function:

$$\mathcal{H}(x) = \begin{cases} 1 & \text{for } x > 0 \\ 0 & \text{for } x = 0 \end{cases} \quad (8)$$

We observe that:

- If all dampers are of the first size then J_p will be equal to $C_{prototype} \times [0 + 1]$;
- If all dampers are of the second size then J_p will be equal to $C_{prototype} \times [1 + 0]$;
- In case dampers of both sizes exist then J_p will be equal to $C_{prototype} \times [1 + 1]$.

2.3 Performance index

We now consider the retrofitting of a generic structure using added dampers. The damage due to earthquakes can be divided into structural and nonstructural. Inter-story drifts, ductility demands in the plastic hinges of structural elements, and hysteretic energy dissipated in these plastic hinges are the responses that indicate structural damage. Ductility demands are strongly associated with the peak inter-story drifts. The contribution of hysteretic energy to common measures of damage is relatively small in most cases. Thus inter-story drifts serve as an appropriate measure of structural damage. Limiting the drifts also allows one to ensure, if feasible, a linear behavior of the structure. This can be assured by limiting the drifts to be smaller than the yield drifts. Moreover, when retrofitting using added dampers, some structures may be designed to behave linearly under certain earthquakes. In these cases structural damage is not expected but non-structural damage should be controlled. In general, non-structural components are sensitive to inter-story drifts and story accelerations. However, in many cases the main cause for their damage is the peak inter-story drift they experience, Charmpis et al. (2012). Hence inter-story drifts are constrained here to allowable values.

The peak inter-story drift normalized by the allowable value is chosen as the local performance index for 2-D frames, defined as

$$d_{c,i} = \max_t (|d_i(t)/d_{all,i}|). \quad (9)$$

Here $d_i(t)$ is the i^{th} inter-story drift and $d_{all,i}$ is the maximum allowable value of $d_i(t)$. For 3-D structures $d_i(t)$ refers to an inter-story drift of a peripheral frame. The $d_i(t)$ performance indices are evaluated through the equations of motion of a linear dynamic viscously damped system, given by:

$$\begin{aligned} \mathbf{M}\ddot{\mathbf{u}}(t) + [\mathbf{C} + \mathbf{C}_d(\mathbf{c}_{d_{TOT}})]\dot{\mathbf{u}}(t) + \mathbf{K}\mathbf{u}(t) &= -\mathbf{M}\mathbf{e}a_g(t) \quad \forall t \\ \mathbf{u}(0) = 0, \quad \dot{\mathbf{u}}(0) &= 0 \end{aligned} \quad (10)$$

where \mathbf{u} is the displacement vector of the degrees of freedom; \mathbf{M} is the mass matrix; \mathbf{K} is the stiffness matrix; \mathbf{C} is the inherent damping matrix; $\mathbf{c}_{d_{TOT}}$ is the added damping vector; \mathbf{C}_d is the supplemental damping matrix; \mathbf{e} is the location vector that defines the location of the excitation; and a_g is the ground acceleration. A linear relation can be defined between the displacements \mathbf{u} and the inter-story drifts \mathbf{d} . In fact $\mathbf{d}(t) = \mathbf{H}\mathbf{u}(t)$, where \mathbf{H} is a transformation matrix (Lavan and Levy (2006)). It should be noted that the present formulation can be extended to the analysis of nonlinear structures and the algorithms considered herein can manage such extension.

2.4 Optimization problem - a mixed formulation

Based on the previous sections, the optimization problem can be stated as follows:

$$\begin{aligned}
& \min_{\mathbf{x}_1, \mathbf{x}_2, \mathbf{y}} \quad J = J_l + J_m + J_p \\
& \text{s. t.} \quad d_{c,i} = \max_t (|d_i(t)/d_{all,i}|) \leq 1 \quad \forall i = 1, \dots, N_{drifts} \\
& \quad x_{1,k} = \{0, 1\} \quad k = 1, \dots, 2N_d \\
& \quad x_{2,k} = \{0, 1\} \quad k = 1, \dots, 2N_d \\
& \quad 0 \leq y_1^L \leq y_1 \leq y_1^U \leq y_2^L \\
& \quad y_1^U \leq y_2^L \leq y_2 \leq y_2^U \leq 1 \\
& \text{with} \quad \mathbf{M}\ddot{\mathbf{u}}(t) + [\mathbf{C} + \mathbf{C}_d(\mathbf{c}_{dTOT})]\dot{\mathbf{u}}(t) + \mathbf{K}\mathbf{u}(t) = -\mathbf{M}\mathbf{e}a_g(t) \quad \forall t, \quad \forall a_g(t) \in \mathcal{E} \\
& \quad \mathbf{u}(0) = 0, \quad \dot{\mathbf{u}}(0) = 0
\end{aligned} \tag{11}$$

where \mathcal{E} is an ensemble of ground motions considered; N_{drifts} is the number of drifts to be constrained; and y_1^L , y_1^U , y_2^L and y_2^U are user-defined bounds. For optimizing the distribution and size of a single damper size-group, only the \mathbf{x}_1 and y_1 variables are necessary, thus it can be seen as a particular case of the two-damper size-group optimization.

The problem (11) was recently solved by the authors using a GA, and it was published in a conference proceedings Pollini et al. (2014). These solutions will be used for comparison hereafter.

3 Continuous approach

In this section we re-formulate the problem (11) using only continuous variables. We utilize material interpolation functions in our formulation in order to reach a practical discrete solution but from a strictly continuous formulation. The interpolation functions essentially penalize intermediate damping coefficients thus giving preference to discrete solutions. Solution of the problem by gradient-based algorithms requires that we rewrite the objective function with continuous variables and continuously differentiable functions. Finally we aggregate the drift constraints into a single constraint, thus approximating the *max* function through a continuous and continuously differentiable function.

3.1 Optimization problem - a continuous formulation

We first reformulate our problem using only continuous variables:

$$\begin{aligned}
& \min_{\mathbf{x}_1, \mathbf{x}_2, \mathbf{y}} \quad J = J_l + J_m + J_p \\
& \text{s. t.} \quad d_{c,i} = \max_t (|d_i(t)/d_{all,i}|) \leq 1 \quad \forall t, \forall i = 1, \dots, N_{drifts} \\
& \quad 0 \leq x_{1,k} \leq 1 \quad k = 1, \dots, 2N_d \\
& \quad 0 \leq x_{2,k} \leq 1 \quad k = 1, \dots, 2N_d \\
& \quad 0 \leq y_1^L \leq y_1 \leq y_1^U \leq y_2^L \\
& \quad y_1^U \leq y_2^L \leq y_2 \leq y_2^U \leq 1 \\
& \text{with} \quad \mathbf{M}\ddot{\mathbf{u}}(t) + [\mathbf{C} + \mathbf{C}_d(\mathbf{c}_{dTOT})]\dot{\mathbf{u}}(t) + \mathbf{K}\mathbf{u}(t) = -\mathbf{M}\mathbf{e}a_g(t) \quad \forall t, \quad \forall a_g(t) \in \mathcal{E} \\
& \quad \mathbf{u}(0) = 0, \quad \dot{\mathbf{u}}(0) = 0
\end{aligned} \tag{12}$$

The variables and the functions involved are the same as in (11), the difference being that in this case we allow the variables $x_{1,k}$ and $x_{2,k}$ to obtain also intermediate values between zero and one.

3.2 Damping penalization

A practical discrete solution starting from a continuous formulation is achieved through the application of well-established material interpolation techniques which have been developed in the last 25 years in the field of structural topology optimization. In classical solid-void topology optimization, the use of

material interpolation schemes such as SIMP (Solid Isotropic Material with Penalization) is the most popular approach and has proven successful for a large number of applications (Bendsøe and Sigmund (2003), Eschenauer and Olhoff (2001)). The idea of relaxing the binary 0-1 problem using penalized intermediate density was originally proposed by Bendsøe (1989). Another material interpolation scheme is RAMP (Rational Approximation of Material Properties) which is similar to the SIMP scheme in its basic concept, Stolpe and Svanberg (2001). The basic idea of these interpolation schemes is to penalize intermediate values of a continuous variable that varies between zero and one; in this way the intermediate values will become uneconomical. This drives the optimized design towards 0-1 solutions (in topology optimization this typically means void or solid). In the problem considered herein there are two vectors of continuous variables \mathbf{x}_1 and \mathbf{x}_2 , whose values vary between zero and one. Both SIMP and RAMP were tested in the formulation of the damping coefficients (1). Similarly to Lavan and Amir (2014), the latter was chosen for the final problem formulation, since it proved to be more effective and promising in achieving final discrete solutions. For optimization with two sizes of dampers, the effective damping coefficients of the two dampers in a potential location j , if they exist, are defined through a multiplication of two RAMP functions:

$$\begin{aligned}\tilde{c}_d(2j-1) &= \bar{c}_d \frac{\mathbf{x}_1(2j-1)}{1+p(1-\mathbf{x}_1(2j-1))} \left(y_1 + (y_2 - y_1) \frac{\mathbf{x}_2(2j-1)}{1+p(1-\mathbf{x}_2(2j-1))} \right); \\ \tilde{c}_d(2j) &= \bar{c}_d \frac{\mathbf{x}_1(2j)}{1+p(1-\mathbf{x}_1(2j))} \left(y_1 + (y_2 - y_1) \frac{\mathbf{x}_2(2j)}{1+p(1-\mathbf{x}_2(2j))} \right).\end{aligned}\tag{13}$$

For $p = 0$, $\tilde{c}_{d_{TOT}}(j) = \tilde{c}_d(2j-1) + \tilde{c}_d(2j)$ is a linear function of \mathbf{x}_1 and \mathbf{x}_2 ; increasing p causes a penalization effect on the intermediate values of \mathbf{x}_1 and \mathbf{x}_2 , thus indirectly leading to a preference for 0-1 solutions. This problem can be generalized to any number of potential damper sizes as suggested by Hvejsel and Lund (2011) in the context of simultaneous topology and multi-material optimization.

3.3 Objective function reformulation

We now present the reformulation of the problem in terms of continuous variables. Some changes need to be introduced in the objective function in order to obtain an effective procedure that is consistent with the definitions made in Section 2. In fact the component of the cost J_p is characterized by a Heaviside step function that needs to be regularized in order to be continuously differentiable. This can be done through the exponential function (e.g. Guest et al. (2004)):

$$\tilde{\mathcal{H}}(x) = 1 - \exp(-\beta x) + x \exp(-\beta).\tag{14}$$

For $\beta = 0$ the function $\tilde{\mathcal{H}}$ is linear, and it tends to match the Heaviside step function as β increases. Fig. 2 displays $\tilde{\mathcal{H}}(x)$ for various values of β , with $0 \leq x \leq 1$. Considering the formulation (14) J_p becomes:

$$\begin{aligned}\tilde{J}_p &= C_{prototype} \left[\tilde{\mathcal{H}}(\mathbf{x}_1^T \mathbf{x}_2 / 2N_d) + \tilde{\mathcal{H}}(\mathbf{x}_1^T (\mathbf{1} - \mathbf{x}_2) / 2N_d) \right] = \\ &= C_{prototype} [(1 - \exp(-\beta \mathbf{x}_1^T \mathbf{x}_2 / 2N_d) + (\mathbf{x}_1^T \mathbf{x}_2 / 2N_d) \exp(-\beta)) + \\ &+ (1 - \exp(-\beta \mathbf{x}_1^T (\mathbf{1} - \mathbf{x}_2) / 2N_d) + (\mathbf{x}_1^T (\mathbf{1} - \mathbf{x}_2) / 2N_d) \exp(-\beta))].\end{aligned}\tag{15}$$

During the analysis the value of the coefficient β grows as the function $\tilde{\mathcal{H}}$ approaches increasingly the Heaviside function. For a small value of β and argument bigger than one, the value of $\tilde{\mathcal{H}}$ might become also bigger than one, something not acceptable. Consequently, the arguments of $\tilde{\mathcal{H}}$ are normalized by their maximum value in Eq. 15. The components J_l and J_m of the cost do not need any modification. We have thus modified the J_p component of the cost, obtaining in this way a cost function \tilde{J} that is continuously differentiable.

3.4 Aggregated constraint

As with the Heaviside function, the *max* function in (12) is also non-differentiable and needs to be replaced with a differentiable function. Similarly to Lavan and Levy (2006), we will use an r-norm

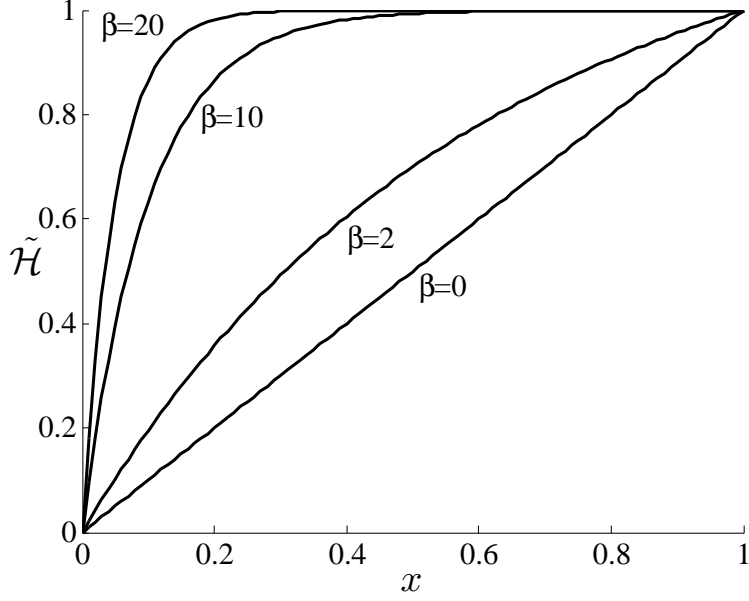


Figure 2: The regularized Heaviside step function for various values of β .

function equivalent to $\max_t(|d_i(t)/d_{all,i}|)$. Thus \mathbf{d}_c is replaced by the approximation:

$$\tilde{\mathbf{d}}_c = \left(\frac{1}{t_f} \int_{t_0}^{t_f} (D^{-1}(\mathbf{d}_{all})D(\mathbf{H}\mathbf{u}(t)))^r dt \right)^{\frac{1}{r}} \mathbf{1}, \quad (16)$$

where r is a large even number. Furthermore, we wish to reduce the number of constraints from N_{drifts} to 1, by aggregating them into a single constraint. The maximal component of $\tilde{\mathbf{d}}_c$ is given by:

$$\tilde{d}_c = \frac{\mathbf{1}^T D^{q+1} \left(\tilde{\mathbf{d}}_c(t_f) \right) \mathbf{1}}{\mathbf{1}^T D^q \left(\tilde{\mathbf{d}}_c(t_f) \right) \mathbf{1}} \quad (17)$$

which is a differentiable weighted average; when q is large this weighted average approaches the value of the maximum component of $\tilde{\mathbf{d}}_c$.

3.5 Final problem formulation and sensitivity analysis

Finally we can present the re-formulation of the optimization problem:

$$\begin{aligned} \min_{\mathbf{x}_1, \mathbf{x}_2, \mathbf{y}} \quad & \tilde{J} = J_l + J_m + \tilde{J}_p \\ \text{s. t.} \quad & \tilde{d}_c = \frac{\mathbf{1}^T D^{q+1} \left(\tilde{\mathbf{d}}_c(t_f) \right) \mathbf{1}}{\mathbf{1}^T D^q \left(\tilde{\mathbf{d}}_c(t_f) \right) \mathbf{1}} \leq 1 \quad \forall \mathbf{a}_g(t) \in \mathcal{E} \\ & 0 \leq x_{1,k} \leq 1 \quad k = 1, \dots, 2N_d \\ & 0 \leq x_{2,k} \leq 1 \quad k = 1, \dots, 2N_d \\ & 0 \leq y_1^L \leq y_1 \leq y_1^U \leq y_2^L \\ & y_1^U \leq y_2^L \leq y_2 \leq y_2^U \leq 1 \\ \text{with} \quad & \mathbf{M}\ddot{\mathbf{u}}(t) + [\mathbf{C} + \mathbf{C}_d(\tilde{\mathbf{c}}_{d_{TOT}})]\dot{\mathbf{u}}(t) + \mathbf{K}\mathbf{u}(t) = -\mathbf{M}\mathbf{e}a_g(t) \quad \forall t, \quad \forall \mathbf{a}_g(t) \in \mathcal{E} \\ & \mathbf{u}(0) = 0, \quad \dot{\mathbf{u}}(0) = 0 \\ & \tilde{\mathbf{d}}_c = \left(\frac{1}{t_f} \int_{t_0}^{t_f} (D^{-1}(\mathbf{d}_{all})D(\mathbf{H}\mathbf{u}(t)))^r dt \right)^{\frac{1}{r}} \mathbf{1} \end{aligned} \quad (18)$$

In order to solve (18) we apply a Sequential Linear Programming approach (SLP), in particular the Cutting Planes Method (Cheney and Goldstein (1959), Kelley (1960)). The sub-problems involved in every optimization cycle make use of first-order derivatives of the objective function and of the general constraint. The gradient of the objective function in (18) is easy to evaluate, while for the gradient of the general constraint an adjoint sensitivity analysis procedure is needed, as presented in Lavan and Levy (2005). In particular after rewriting (18) with the state space formulation, the gradient of the general constraint ($\tilde{d}_c - 1 \leq 0$) is obtained by first writing the augmented objective function of a secondary minimization problem of the general constraint. The variation of this augmented objective function results in a set of differential equations and final boundary conditions to be satisfied, when all multipliers of the variations (except $\delta_{\tilde{c}_{d_{TOT}}}$) are set to zero. The multiplier of the variation $\delta_{\tilde{c}_{d_{TOT}}}$ will yield the expression for the evaluation of the gradient $\nabla_{\tilde{c}_{d_{TOT}}} \tilde{d}_c$. This procedure thus allows us to compute the sensitivity of the aggregated drift constraint with respect to the total physical damping coefficient at a certain location j (i.e. $\frac{\partial \tilde{d}_c}{\partial \tilde{c}_{d_{TOT},j}}$). Then the complete sensitivity is computed by the chain rule:

$$\begin{aligned}
\frac{\partial \tilde{d}_c}{\partial x_{1,2j-1}} &= \frac{\partial \tilde{d}_c}{\partial \tilde{c}_{d_{TOT},j}} \frac{\partial \tilde{c}_{d,2j-1}}{\partial x_{1,2j-1}}; & \frac{\partial \tilde{d}_c}{\partial x_{2,2j-1}} &= \frac{\partial \tilde{d}_c}{\partial \tilde{c}_{d_{TOT},j}} \frac{\partial \tilde{c}_{d,2j-1}}{\partial x_{2,2j-1}}; \\
\frac{\partial \tilde{d}_c}{\partial x_{1,2j}} &= \frac{\partial \tilde{d}_c}{\partial \tilde{c}_{d_{TOT},j}} \frac{\partial \tilde{c}_{d,2j}}{\partial x_{1,2j}}; & \frac{\partial \tilde{d}_c}{\partial x_{2,2j}} &= \frac{\partial \tilde{d}_c}{\partial \tilde{c}_{d_{TOT},j}} \frac{\partial \tilde{c}_{d,2j}}{\partial x_{2,2j}}; \\
\frac{\partial \tilde{d}_c}{\partial y_1} &= \sum_{j=1}^{N_d} \frac{\partial \tilde{d}_c}{\partial \tilde{c}_{d_{TOT},j}} \left(\frac{\partial \tilde{c}_{d,2j-1}}{\partial y_1} + \frac{\partial \tilde{c}_{d,2j}}{\partial y_1} \right); & & (19) \\
\frac{\partial \tilde{d}_c}{\partial y_2} &= \sum_{j=1}^{N_d} \frac{\partial \tilde{d}_c}{\partial \tilde{c}_{d_{TOT},j}} \left(\frac{\partial \tilde{c}_{d,2j-1}}{\partial y_2} + \frac{\partial \tilde{c}_{d,2j}}{\partial y_2} \right). & &
\end{aligned}$$

3.6 Algorithm implementation

As mentioned above, the optimization problem has been solved using a Cutting Planes procedure. This approach is typically used to solve nonlinear convex problems. As the problem under consideration is both highly nonconvex and nonlinear, some precautions are needed when implementing the proposed approach.

Selection of the ground motion. In general all the ground motions in the ensemble should be considered in every design cycle, but such an approach would not be very efficient. A good choice of the ground motion is one for which it remains an active constraint at the optimal solution during the process. Active means that the excitation caused by a particular ground motion pushes the structure to its limits, or close to them, during the entire optimization process more than the other ground motions in the ensemble. In this work, since displacements are constrained, the record with the maximal spectral displacement has been selected. Once the optimization with this ground motion is concluded, additional ground motions from the ensemble are considered if the constraint is violated with one of them. The optimization and the constraint verification repeat until the optimal solution satisfies the constraint with all the records from the ensemble.

Managing the constraints. In the Cutting Planes Method, within each optimization cycle a linear sub-problem is generated and solved. Within every design cycle, a new linearized constraint is added so the linear sub-problem expands. In our case we are solving a nonconvex problem and it may happen that some of the linearized constraints might be active even though the solution is well located within the feasible domain, thus enforcing too conservative solutions. In such cases these constraints are nullified and deleted in the following cycles, as proposed in Lavan and Levy (2005).

Conservative approach. The optimization problem (18) includes several components that make the problem highly nonlinear and nonconvex: the penalized damping, the aggregated constraint and the Heaviside functions in the objective. Thus finding a good optimized solution may be difficult. In order to converge gradually to an optimized solution, the penalizing parameter p , the parameters q and r of the aggregated

constraint, the components of the cost \mathbf{C}_{m1} , \mathbf{C}_{m2} , and $C_{prototype}$, and the parameter β of the Heaviside functions are increased gradually to their final values according to certain measures of the convergence of the solution. Moreover, conservative move limits are also considered, limiting the feasible domains of \mathbf{x}_1 , \mathbf{x}_2 , y_1 , and y_2 to a small neighborhood of the solution of the previous sub-problem within the design iterations. Specific details regarding these settings will be given in the description of the numerical examples.

4 Numerical examples

In this section we present and discuss several results obtained by solving the optimization problem presented in the previous sections. As mentioned above, the continuous formulation (18) was solved by an SLP approach – particularly the Cutting Planes method – implemented in MATLAB by the authors. The mixed-integer formulation (11) was solved using MATLAB’s built-in GA. Based on the performance of the two implementations, the formulations are compared in terms of the results achieved and of the computational effort that was invested.

In particular we consider two examples of asymmetric frames made of reinforced concrete, as introduced in Tso and Yao (1994). These two test cases were also solved in Lavan and Levy (2006), where an optimal continuous damping was found, and in Lavan and Amir (2014) but yielding a discrete damping distribution. In both examples the column sizes are $0.5\text{ m} \times 0.5\text{ m}$ in frames 1 and 2; $0.7\text{ m} \times 0.7\text{ m}$ in frames 3 and 4 (see Fig.3 and Fig.10). The beam sizes are $0.4\text{ m} \times 0.6\text{ m}$ and the floor mass is uniformly distributed with a weight of $0.75\text{ [ton/m}^2\text{]}$. Regarding the ground motion acceleration, out of the ensemble $LA\ 10\%$ in 50 years (National Information Service for Earthquake Engineering - University of California, Berkeley (NA)), $LA16$ has the largest maximal displacement for reasonable values of the periods of the structures in both examples. Hence $LA16$ was the ground motion to be considered first in both examples, acting in the y direction, Lavan and Levy (2006). In the present work, we consider 5% of critical damping for the first two modes in order to build the Rayleigh damping matrix of the structures.

4.1 Eight-story three bay by three bay asymmetric structure

A plan and two sections of the first frame to be optimized are displayed in Fig. 3. Based on the results of Lavan and Levy (2006), 16 potential locations for dampers were assigned at the exterior frames in the y direction. The allowable inter-story drift was set to 0.035 m . The maximum nominal damping coefficient was set to $\bar{c}_d = 50,000\text{ [kNs/m]}$.

In the SLP solution, the penalizing coefficient p of the added damping was increased gradually from 0.1 up to 100. The coefficients of the cost \mathbf{C}_{m1} , \mathbf{C}_{m2} and $C_{prototype}$ were gradually increased by the coefficient s so that: $\mathbf{C}_{m1} = s\bar{\mathbf{C}}_{m1}$, $\mathbf{C}_{m2} = s\bar{\mathbf{C}}_{m2}$ and $C_{prototype} = s\bar{C}_{prototype}$; s varied from 0.1 to 1. For $s = 1$, $\mathbf{C}_{m1} = 20,000 \cdot [1\ 0\ 1\ 0\ \dots]^T\text{ [kNs/m]}$, $\mathbf{C}_{m2} = 10,000 \cdot [0\ 1\ 0\ 1\ \dots]^T\text{ [kNs/m]}$ and $C_{prototype} = 10,000\text{ [kNs/m]}$. Also the coefficient β of the Heaviside functions was increased via the parameter s : For $s = 1$, $\beta = 100$. The coefficients r and q of the aggregated constraint increased from a value of 100 with steps of 20 during the optimization process. The variables were bounded as follows: $0 \leq \mathbf{x}_1 \leq 1$, $0 \leq \mathbf{x}_2 \leq 1$, $0 \leq y_1 \leq 0.5$ and $0.5 \leq y_2 \leq 1$; a move limit of 0.1 was considered. We defined four criteria for convergence to be satisfied simultaneously: The first two require the parameters p and s to reach their maximum values; The third requires the damping coefficients between two consecutive iterations to be similar with a tolerance of 1% ; The fourth requires all the actual drifts to be smaller than the allowable value with a tolerance of 1% . The process converged after 461 iterations in MATLAB. The values $y_1 = 0.4573$ and $y_2 = 0.6692$ were obtained, corresponding to the damping coefficients $\bar{c}_1 = 22,863\text{ [kNs/m]}$ and $\bar{c}_2 = 33,459\text{ [kNs/m]}$. The optimized solution, in terms of the values of \mathbf{x}_1 and \mathbf{x}_2 , was not precisely binary so that some rounding was needed. The original and rounded off optimized solutions are presented in Tab. 1.

The optimized damper size and distribution in the potential locations considering the rounded optimal \mathbf{x}_1 and \mathbf{x}_2 are shown in Fig. 4. Fig. 5 shows the drift distribution in the optimized structure. One slight violation occurs in location number 10 where the drift exceeds the allowable value by 0.40% (or 0.014 cm). Finally, the optimized solution obtained by the SLP procedure was tested with the other ground motions from the ensemble. None of the other records caused any violation of the drift constraint.

k^{th} damper location	$\mathbf{x}_1(2k-1), \mathbf{x}_1(2k)$	$\mathbf{x}_2(2k-1), \mathbf{x}_2(2k)$	$\mathbf{x}_1^{rounded}(2k-1), \mathbf{x}_1^{rounded}(2k)$	$\mathbf{x}_2^{rounded}(2k-1), \mathbf{x}_2^{rounded}(2k)$
1	0, 0	N/A, N/A	0, 0	N/A, N/A
2	1, 0.1027	1, 1	1, 0	1, N/A
3	1, 0	0, N/A	1, 0	0, N/A
4	1, 0	0, N/A	1, 0	0, N/A
5	0.9936, 0	0, N/A	1, 0	0, N/A
6-9	0, 0	N/A, N/A	0, 0	N/A, N/A
10	1, 0.0883	0, 0	1, 0	0, N/A
11	1, 0	1, N/A	1, 0	1, N/A
12	0.999, 0	0, N/A	1, 0	0, N/A
13-16	0, 0	N/A, N/A	0, 0	N/A, N/A

Table 1: Optimal values of \mathbf{x}_1 and \mathbf{x}_2 achieved with the SLP in Ex. 4.1 considering first only the record LA16. The values of \mathbf{x}_2 not associated to an existing damper are irrelevant, and replaced with N/A (not applicable).

In the GA implementation the following parameters were used: $\mathbf{C}_{m1} = 20,000 \cdot [1\ 0\ 1\ 0 \dots]^T$ [kNs/m]; $\mathbf{C}_{m2} = 10,000 \cdot [0\ 1\ 0\ 1 \dots]^T$ [kNs/m]; and $C_{prototype} = 10,000$ [kNs/m]. The population size was set to 500. In order to guarantee the convergence of the algorithm to a global optimum with high probability, 20 different analyses were performed, of which the best solution was chosen. The variables were bounded as follows: $\mathbf{x}_1 = \{0, 1\}$, $\mathbf{x}_2 = \{0, 1\}$, $0 \leq y_1 \leq 0.5$ and $0.5 \leq y_2 \leq 1$. In this case we defined two criteria for convergence: The first halts the algorithm when the number of generations (i.e. iterations) reaches the maximum number allowable *Generatons* – 800; The second halts the algorithm when the weighted average relative change in the best fitness function value over *StallGenLimit* generations is less than or equal to *TolFun*. *StallGenLimit* is an integer set to 300, and *TolFun* is a positive scalar set to 1^{-10} . The process converged after 301 iterations in MATLAB. The values $y_1 = 0.3236$ and $y_2 = 0.6039$ were obtained, corresponding to the damping coefficients $\bar{c}_1 = 16,180$ [kNs/m] and $\bar{c}_2 = 30,198$ [kNs/m]. The optimized damper sizes and the distribution in the potential locations are shown in Fig. 6. Fig. 7 shows the drift distribution for the optimized damper distribution.

The solutions achieved with the two methods are characterized by similar final costs and the same topologies. In fact the two algorithms chose to distribute the dampers in the same locations. The solutions differ in the optimized sizes of the dampers’ groups and in the total damping added in each location. This can be justified by the high non-convexity of the problem that causes the presence of several local minima in proximity of the global optima. The main advantage in solving this optimization problem with a gradient based approach is the significant reduction in computational effort needed to achieve a good solution, compared to that of a GA. To get a satisfying solution with a GA we need to consider a big population and to repeat several times the optimization analysis. In this case we considered a population of 500 individuals, meaning that the algorithm performed 500 time history analyses in each iteration, and we repeated the optimization process 20 times. On the other hand, the SLP needed to compute two time history analyses each iteration for just one optimization process: one for the structural response and one for the evaluation of the constraint gradient. The final solution of the SLP is also characterized by a small constraint violation, since the SLP solves a series of linear approximations of (18). For a synoptic comparison of the results and performances of the two approaches please refer to Tab. 2.

	\tilde{J}, J [kNs/m]	$d_{c,max}/d_{all}$	\bar{c}_{d1} [kNs/m]	\bar{c}_{d2} [kNs/m]	Func. evaluations (gradient evaluations are included as function evaluations in the SLP)
SLP	341,216	1.0040 (0.40%)	22,863	33,459	$2 \cdot 461 \approx 10^{2.965}$
GA	341,495	1 (0.00%)	16,180	30,198	$20 \cdot 500 \cdot 301 \approx 10^{6.478}$

Table 2: Synthetic comparison of the solutions achieved with the SLP and the GA in Ex. 4.1 considering only LA16. Compared to the GA, the SLP provides a solution with a very similar final cost, a very small constraint violation, while requiring a computational effort smaller almost by four orders of magnitude.

In order to further explore the capabilities of the new cost function we performed another analysis with the SLP considering the same structure, this time increasing the component of the cost $C_{prototype}$ from 10,000 [kNs/m] to 50,000 [kNs/m]. Clearly it is expected that the algorithm will choose a distribution

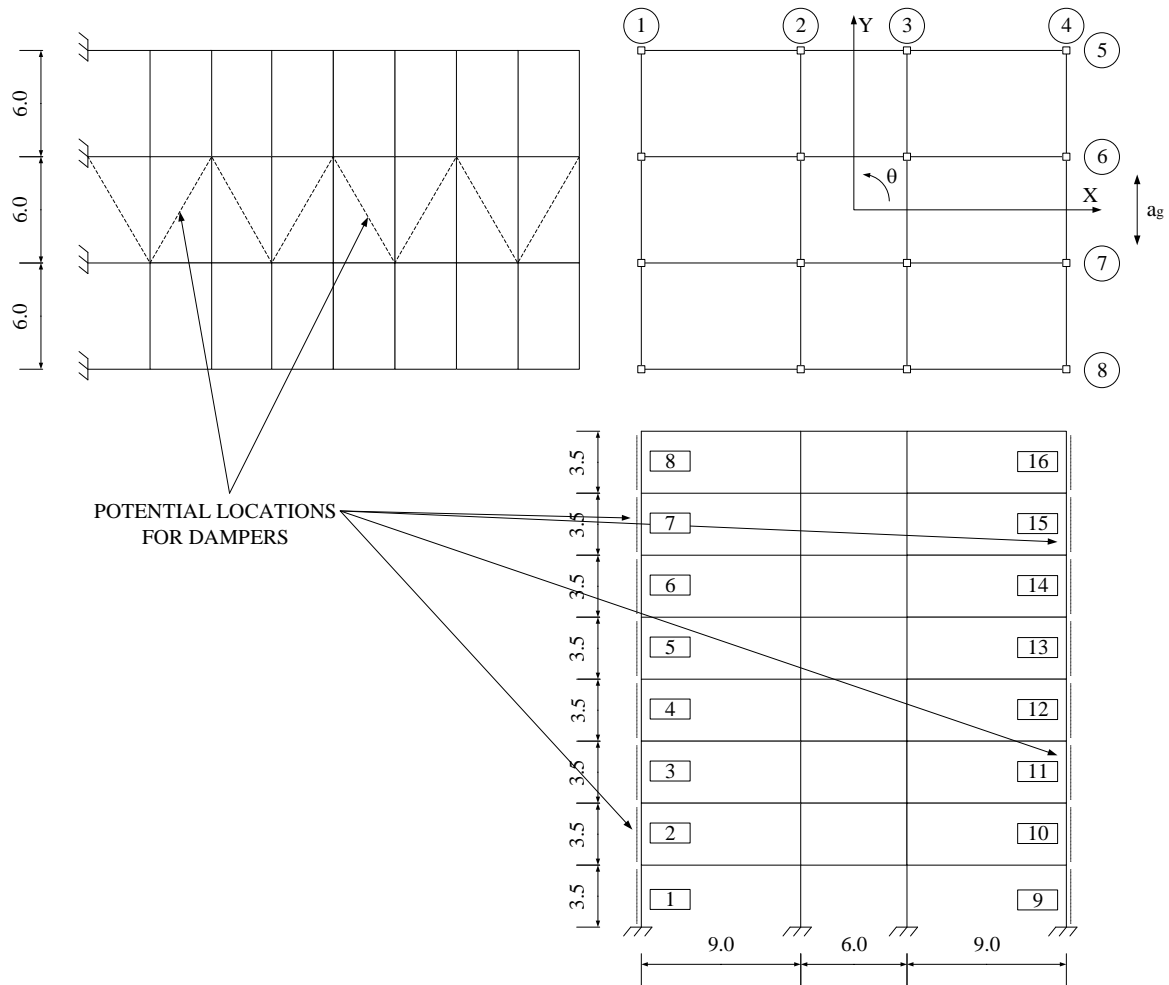


Figure 3: Scheme of the asymmetric 3-D frame considered in Ex. 4.1. The lengths are in meters.

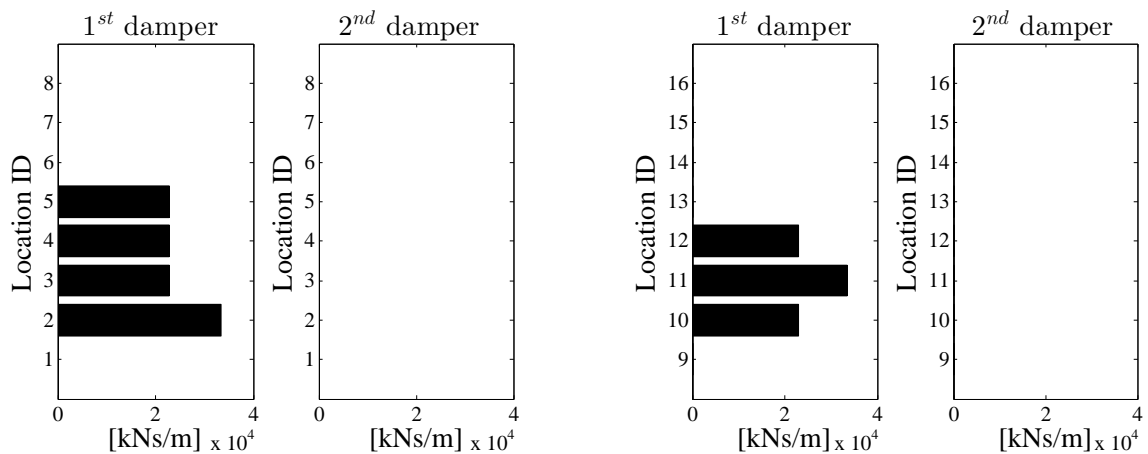


Figure 4: SLP solution. First and second damper for each location in Ex. 4.1 considering first only the record LA16. The solution involves dampers of both the size-groups, and in the same potential locations chosen by the GA (Fig. 6).

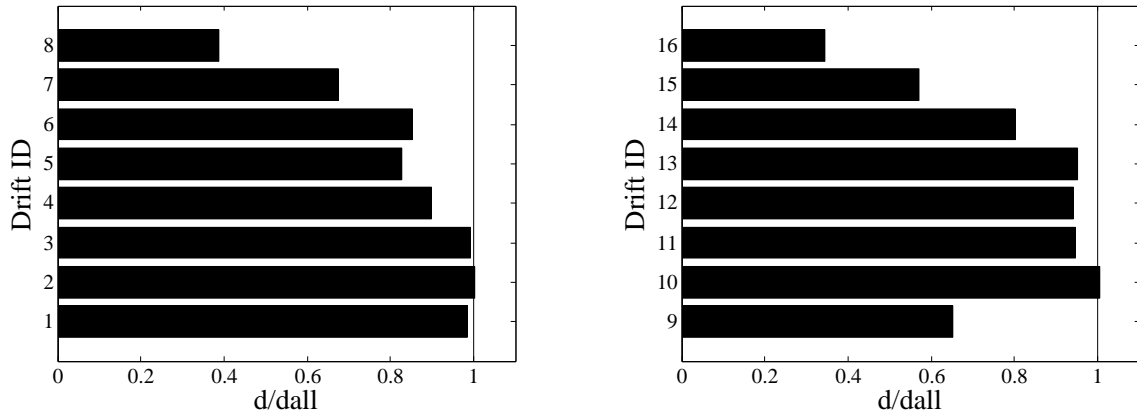


Figure 5: SLP solution. Drift distribution in Ex. 4.1 considering first only the record *LA16*. The drift number 10 exceeds the allowable value by the 0.40%.

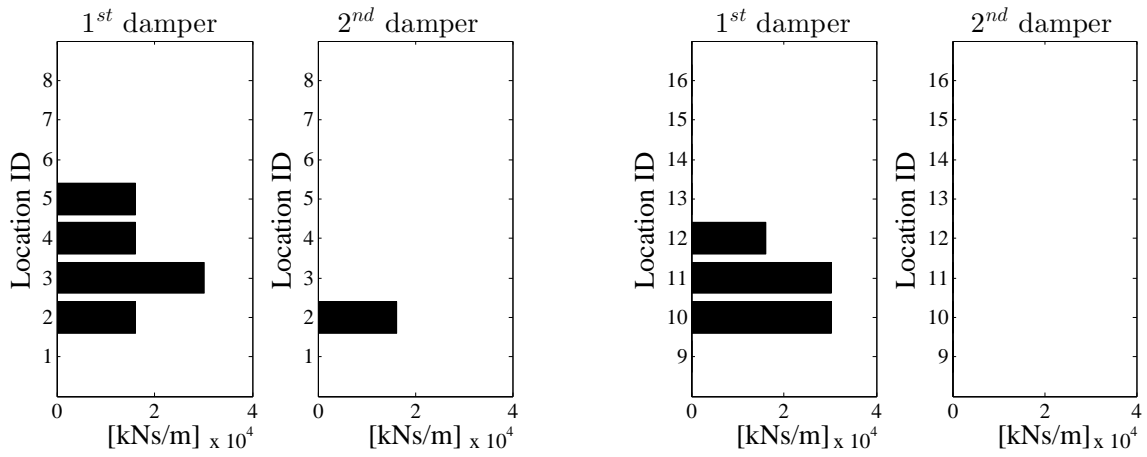


Figure 6: GA solution. First and second damper for each location in Ex. 4.1 considering first only *LA16*. The solution involves dampers of both the available size-groups, and in the same potential locations chosen by the SLP (Fig. 4).

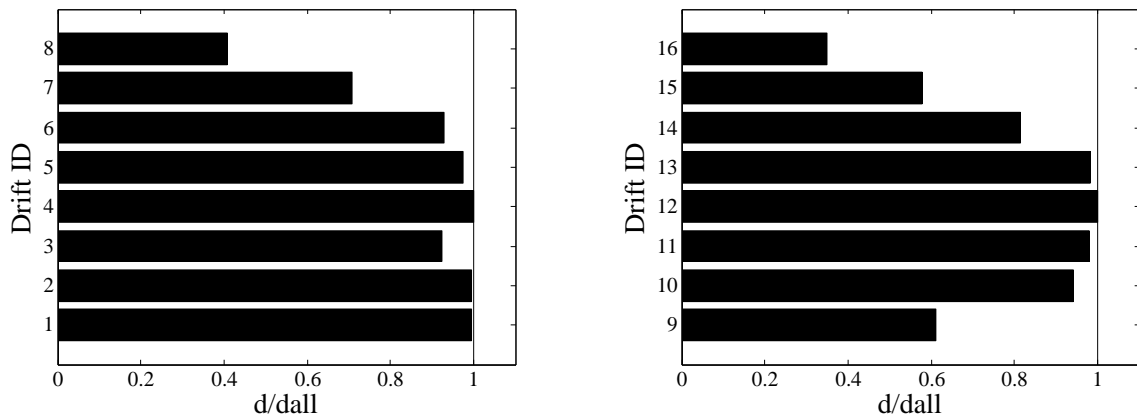


Figure 7: GA solution. Drift distribution in Ex. 4.1 considering first only *LA16*. There is no constraint violation.

of dampers of a single size-group. This time in the SLP the penalizing coefficient p of the added damping was increased gradually from 0.7 up to 100, and the coefficients r and q of the aggregated constraint grew with steps of 50 starting from a value of 100. These modifications are required to converge to a binary solution otherwise more complicated to achieve. All other parameters were not modified, including the criteria for convergence. The process converged after 178 iterations in MATLAB. Examining the values obtained for \mathbf{x}_1 and \mathbf{x}_2 as presented in Tab. 3, it can be seen that these are not precisely binary. Therefore, some simple rounding is needed in order to interpret the result to a practical engineering solution, as presented in the 4th and 5th columns in Tab. 3. Most importantly, the interpreted design consists of only one damper size – as expected due to the high cost related to prototype testing. The optimization procedure yielded values of $y_1 = 0.3212$ and $y_2 = 0.9701$ which correspond to the damping coefficients $\bar{c}_1 = 16,058$ [kNs/m] and $\bar{c}_2 = 48,503$ [kNs/m]. However, only dampers of type $\bar{c}_1 = 16,058$ [kNs/m] are actually allocated.

k^{th} damper location	$\mathbf{x}_1(2k-1), \mathbf{x}_1(2k)$	$\mathbf{x}_2(2k-1), \mathbf{x}_2(2k)$	$\mathbf{x}_1^{rounded}(2k-1), \mathbf{x}_1^{rounded}(2k)$	$\mathbf{x}_2^{rounded}(2k-1), \mathbf{x}_2^{rounded}(2k)$
1	0, 0	N/A, N/A	0, 0	N/A, N/A
2	1, 1	0, 0	1, 1	0, 0
3	1, 1	0, 0	1, 1	0, 0
4	1, 0	0, N/A	1, 0	0, N/A
5	0.9996, 0	0, N/A	1, 0	0, N/A
6-9	0, 0	N/A, N/A	0, 0	N/A, N/A
10	1, 0.9947	0, 0	1, 1	0, 0
11	1, 1	0, 0	1, 1	0, 0
12	1, 0	0, N/A	1, 0	0, N/A
13-16	0, 0	N/A, N/A	0, 0	N/A, N/A

Table 3: Optimal values of \mathbf{x}_1 and \mathbf{x}_2 achieved with the SLP in Ex. 4.1 with $C_{prototype} = 50,000$ [kNs/m]. The values of \mathbf{x}_2 not associated to an existing damper are irrelevant, and replaced with N/A (not applicable).

The optimized damper size and distribution in the potential locations considering the rounded optimized \mathbf{x}_1 and \mathbf{x}_2 are shown in Fig. 8. Fig. 9 shows the drift distribution for the optimized damper distribution. The drift in the location number 1 violated the allowable value by the 0.08% (or 0.0028 cm). Finally, the optimized design solution was checked with all other records from the ensemble. None of the maximum values of the drifts exceeded the allowable value.

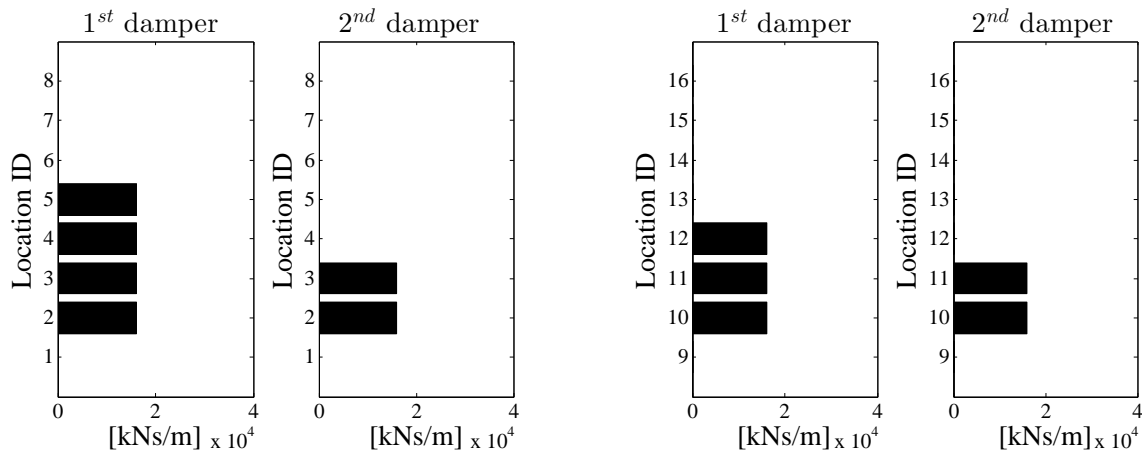


Figure 8: SLP solution. First and second damper for each location in Ex. 4.1 with $C_{prototype} = 50,000$ [kNs/m] and considering first only LA16. Only dampers of the first size-group ($\bar{c}_1 = 16,058$ [kNs/m]) are actually allocated.

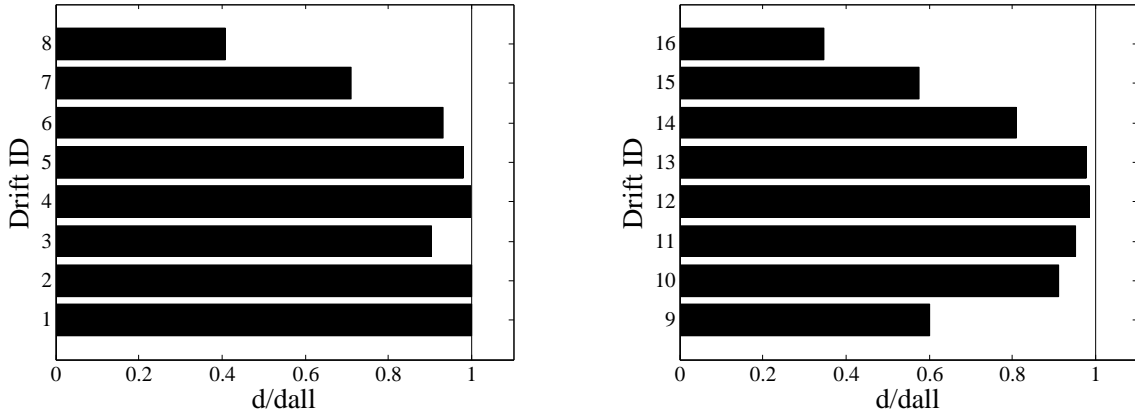


Figure 9: SLP solution. Drift distribution in Ex. 4.1 with $C_{prototype} = 50,000 [kNs/m]$ and considering first only *LA16*. The drift number 1 exceeds the allowable value by the 0.08%.

	\tilde{J} [kNs/m]	$d_{c,max}/d_{all}$	\bar{c}_{d1} [kNs/m]	\bar{c}_{d2} [kNs/m]	Func. evaluations (gradient evaluations are included as function evaluations in the SLP)
SLP	406,640	1.0008 (0.08%)	16,058	N/A	$2 \cdot 178 \approx 10^{2.551}$

Table 4: Summary of the results attained with the SLP in Ex. 4.1 with $C_{prototype} = 50,000 [kNs/m]$ and considering first only the record *LA16*. Only dampers of size $\bar{c}_1 = 16,058 [kNs/m]$ are actually allocated.

4.2 Eight-story three bay by three bay setback structure

In the second example we consider a similar 3-D frame structure but with a setback – the top 4 stories in frames 1 and 2 are omitted. A plan and two sections of the frame are displayed In Fig. 10. Again, 16 potential locations for dampers were assigned at the exterior frames in the y direction (Lavan and Levy (2006)), and the allowable inter-story drift was set to $0.035 m$. The maximum nominal damping coefficient was set to $\bar{c}_d = 50,000 [kNs/m]$.

In the SLP procedure, the penalizing coefficient p of the added damping was increased gradually from 0.1 up to 100. The coefficients of the cost \mathbf{C}_{m1} , \mathbf{C}_{m2} and $C_{prototype}$ were multiplied by the coefficient s such that: $\mathbf{C}_{m1} = s\bar{\mathbf{C}}_{m1}$, $\mathbf{C}_{m2} = s\bar{\mathbf{C}}_{m2}$ and $C_{prototype} = s\bar{C}_{prototype}$; s varied from 0.1 to 1. For $s = 1$, $\mathbf{C}_{m1} = 20,000 \cdot [1\ 0\ 1\ 0 \dots]^T [kNs/m]$, $\mathbf{C}_{m2} = 10,000 \cdot [0\ 1\ 0\ 1 \dots]^T [kNs/m]$ and $C_{prototype} = 10,000 [kNs/m]$. Also the coefficient β of the Heaviside functions was increased in conjunction with the parameter s , so that for $s = 1$, $\beta = 100$. The coefficients r and q of the aggregated constraint increased from a value of 100 with steps of 50 during the optimization process. The variables were bounded as follows: $0 \leq \mathbf{x}_1 \leq 1$, $0 \leq \mathbf{x}_2 \leq 1$, $0 \leq y_1 \leq 0.5$ and $0.5 \leq y_2 \leq 1$. Finally, a move limit of 0.1 was imposed, and the criteria for convergence were the same as in the previous example. The optimization process converged after 276 iterations in MATLAB. The values $y_1 = 0.0825$ and $y_2 = 0.5413$ were obtained, corresponding to the damping coefficients $\bar{c}_1 = 4,126 [kNs/m]$ and $\bar{c}_2 = 27,067 [kNs/m]$. In the optimal solution only dampers of size $\bar{c}_2 = 27,067$ are actually distributed. The optimized solution as reflected in the relevant values of \mathbf{x}_1 and \mathbf{x}_2 was exactly binary and in this case the rounding was not necessary, as can be seen in Tab. 5.

The optimized damper size and distribution in the potential locations considering the rounded optimized \mathbf{x}_1 and \mathbf{x}_2 are shown in Fig. 11. Fig. 12 shows the drift distribution for the optimized dampers distribution. The only violation occurs in location 12 where the drift exceeds the allowable value by 0.06% (or 0.0021 cm).

In the GA solution of the same example the parameters were set as follows: $\mathbf{C}_{m1} = 20,000 \cdot [1\ 0\ 1\ 0 \dots]^T [kNs/m]$, $\mathbf{C}_{m2} = 10,000 \cdot [0\ 1\ 0\ 1 \dots]^T [kNs/m]$ and $C_{prototype} = 10,000 [kNs/m]$. The population size was set to 500 and the maximum number of iterations was set to 800. In order to guarantee convergence of the algorithm to a global optimum with a high probability, 20 different analyses were performed, of

k^{th} damper location	$\mathbf{x}_1(2k-1), \mathbf{x}_1(2k)$	$\mathbf{x}_2(2k-1), \mathbf{x}_2(2k)$	$\mathbf{x}_1^{rounded}(2k-1), \mathbf{x}_1^{rounded}(2k)$	$\mathbf{x}_2^{rounded}(2k-1), \mathbf{x}_2^{rounded}(2k)$
1	0, 0	N/A, N/A	0, 0	N/A, N/A
2	1, 0	1, N/A	1, 0	1, N/A
3-9	0, 0	N/A, N/A	0, 0	N/A, N/A
10	1, 0	1, N/A	1, 0	1, N/A
11	1, 0	1, N/A	1, 0	1, N/A
12-16	0, 0	N/A, N/A	0, 0	N/A, N/A

Table 5: Optimal values of \mathbf{x}_1 and \mathbf{x}_2 achieved with the SLP in Ex. 4.2 considering first only the record LA16. The values of \mathbf{x}_2 not associated to an existing damper are irrelevant, and replaced with N/A (not applicable).

which the superior solution was chosen. The variables were bounded as follows: $\mathbf{x}_1 = \{0, 1\}$, $\mathbf{x}_2 = \{0, 1\}$, $0 \leq y_1 \leq 0.5$ and $0.5 \leq y_2 \leq 1$. The criteria for convergence were the same as in the previous example. The process converged after 301 iterations in MATLAB. The values $y_1 = 0.3043$ and $y_2 = 0.5487$ were obtained, corresponding to the damping coefficients $\bar{c}_1 = 15,217 [kNs/m]$ and $\bar{c}_2 = 27,438 [kNs/m]$. The optimized damper size and distribution in the potential locations are shown in Fig. 13. Fig. 14 shows the drift distribution for the optimized damper distribution.

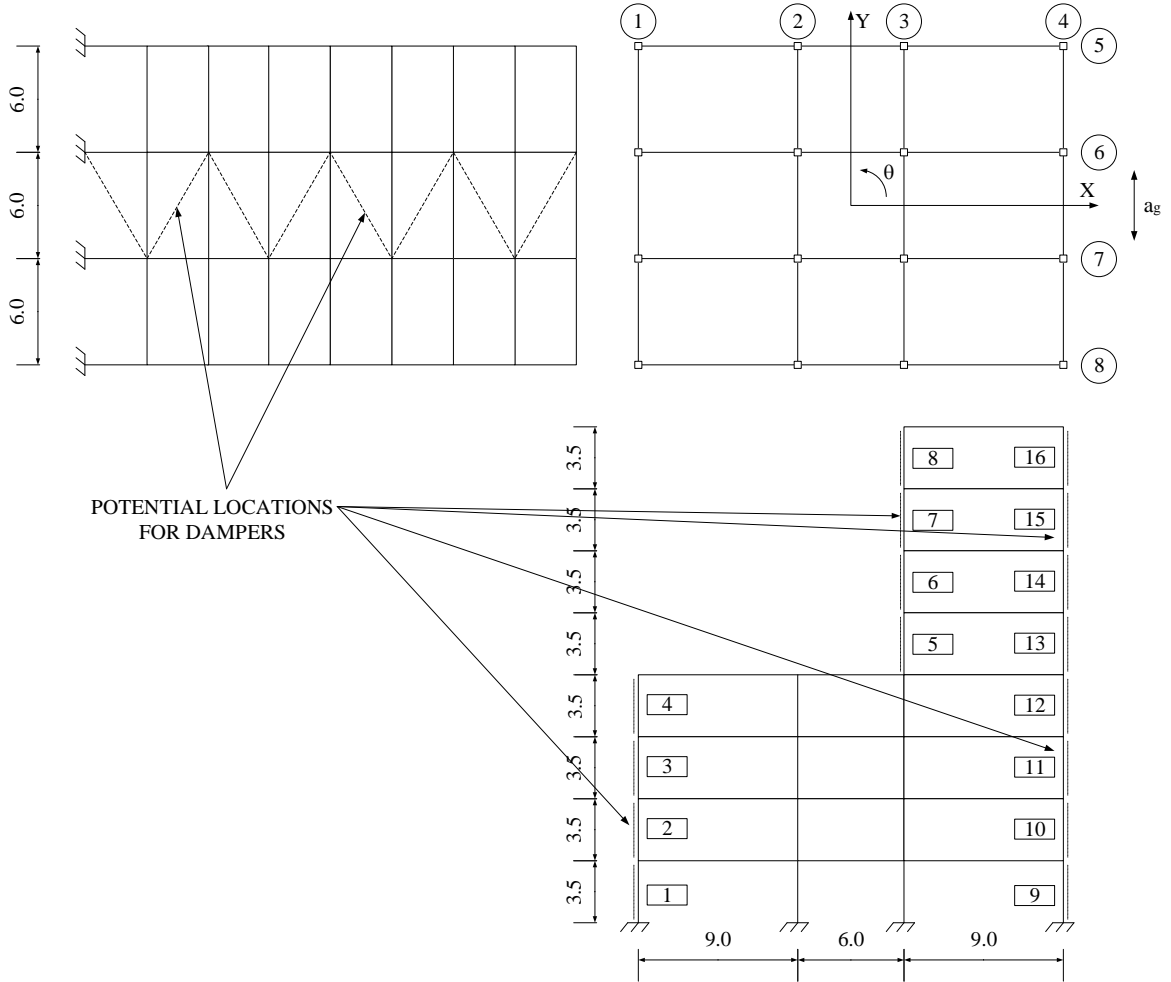


Figure 10: Scheme of the asymmetric 3-D frame considered in Ex. 4.2. The lengths are in meters.

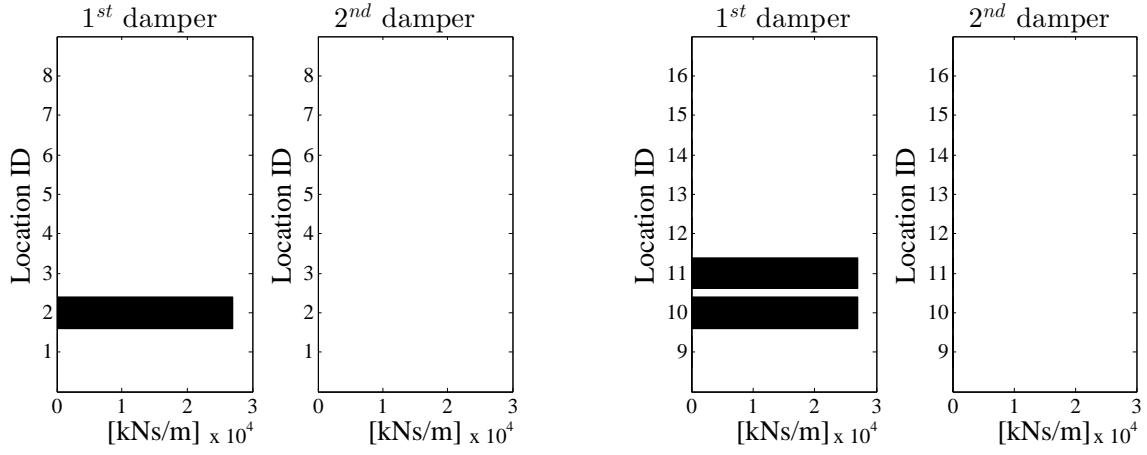


Figure 11: SLP solution. First and second damper for each location in Ex. 4.2 considering first only the record *LA16*. The solution involves only dampers of the second size-group ($\bar{c}_2 = 27,067 [kNs/m]$) in the same potential locations chosen by the GA (Fig. 13).

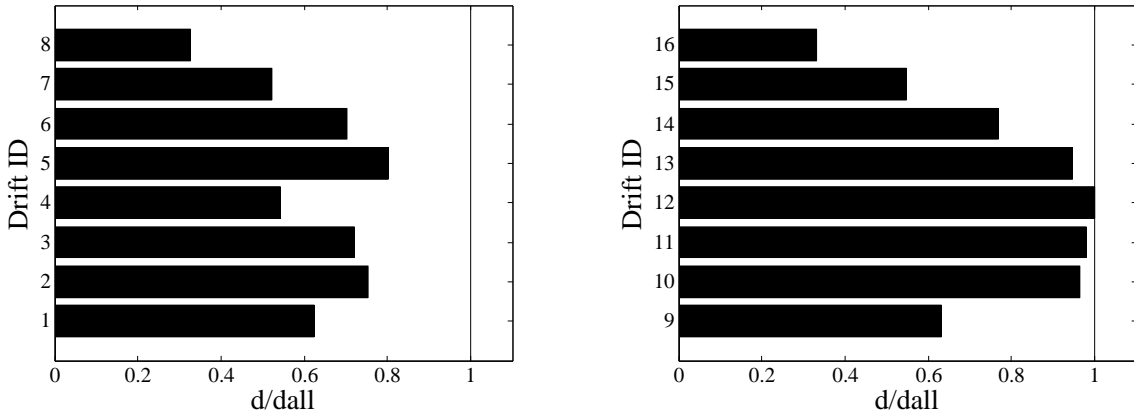


Figure 12: SLP solution. Drift distribution in Ex. 4.2 considering first only the record *LA16*. The drift number 12 exceeds the allowable value by the 0.06%.

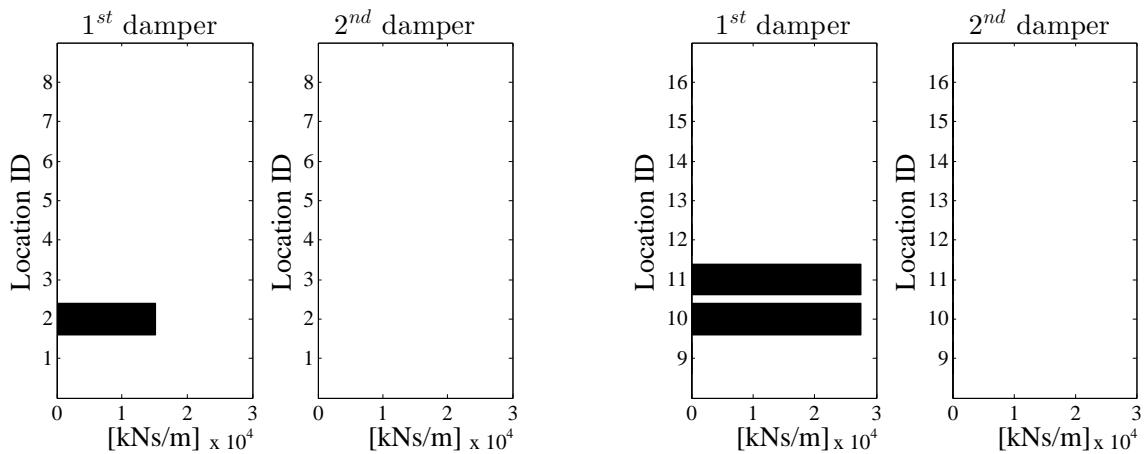


Figure 13: GA solution. First and second damper for each location in Ex. 4.2 considering first only *LA16*. The solution involves dampers of both the available size-groups in the same potential locations chosen by the SLP (Fig. 11).

Also in this example the two solutions were very similar in terms of final costs, identical looking at the optimal topologies, and different in terms of the total added damping for each potential location.

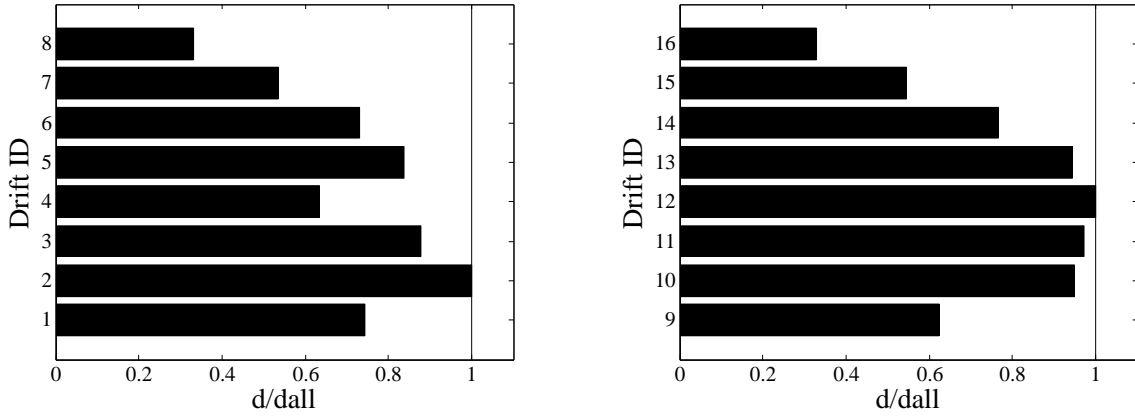


Figure 14: GA solution. Drift distribution in Ex. 4.2 considering first only *LA16*. There is no constraint violation.

The computational effort required by the SLP to achieve the solution was also in this case much smaller than that of the GA. Looking at the Function Evaluations of Tab. 6 it is possible to verify that the ratio between the computational efforts of the SLP and of the GA is approximately 1 : 5000. Also in this case the GA needed to execute 500 time history analyses in each iteration, for 20 different optimization processes, while the SLP needed to perform only two analyses in each iteration for the same reasons mentioned in Ex. 4.1. The solution achieved with SLP still slightly violates the constraint because of the linear approximation of (18). To compare the results and performances of the two approaches please refer to Tab. 6.

	\tilde{J}, J [kNs/m]	$d_{c,max}/d_{all}$	\bar{c}_{d1} [kNs/m]	\bar{c}_{d2} [kNs/m]	Func. evaluations <small>(gradient evaluations are included as function evaluations in the SLP)</small>
SLP	151,202	1.0006 (0.06%)	N/A	27,067	$2 \cdot 276 \approx 10^{2.742}$
GA	150,093	1 (0.00%)	15,217	27,438	$20 \cdot 500 \cdot 301 \approx 10^{6.478}$

Table 6: Synthetic comparison of the solutions achieved with the SLP and the GA in Ex. 4.2 considering first only *LA16*. In the solution of SLP only dampers of size $\bar{c}_2 = 27,067$ [kNs/m] are actually allocated.

The optimized rounded solution obtained by the SLP procedure was tested with the other ground motions from the *LA* 10% in 50 years ensemble. With two of the records, namely *LA14* and *LA18*, a constraint violation was encountered. Since *LA14* had the largest constraint violation (see Tab. 7), another optimization process was initiated with both *LA16* and *LA14* considered as ground excitations.

Record	$\max(d_{c,i}/d_{all})$	Record	$\max(d_{c,i}/d_{all})$
LA01	0.6015	LA11	0.6141
LA02	0.8066	LA12	0.7724
LA03	0.5103	LA13	0.9918
LA04	0.4173	LA14	1.0411
LA05	0.3475	LA15	0.8188
LA06	0.3065	LA16	1.0006
LA07	0.4108	LA17	0.6152
LA08	0.4600	LA18	1.0123
LA09	0.7030	LA19	0.8117
LA10	0.4420	LA20	0.8106

Table 7: Maximum $d_{c,max}/d_{all}$ for each record from *LA* 10% in 50 years evaluated considering the structure with the optimal distribution of dampers. This distribution is the one achieved with the SLP considering only *LA16* in Ex. 4.2.

In this case, the penalizing coefficient p of the added damping was increased gradually from 0.7 up to 150. When considering two ground motions simultaneously, it becomes more problematic to achieve a binary solution that does not need much final rounding. Therefore, the final value of the penalizing coefficient assumes an important role for a good convergence of the problem: raising it to 150 helps converging very close to a binary solution. All other parameters were set as before, including the criteria for convergence. The process converged after 197 iterations in MATLAB, with a final cost $\tilde{J} = 184,018$ [kNs/m]. The values $y_1 = 0.1603$ and $y_2 = 0.5$ were obtained, corresponding to the damping coefficients $\bar{c}_1 = 8,013$ [kNs/m] and $\bar{c}_2 = 25,000$ [kNs/m]. Looking at the solution, it appeared that the algorithm tried to reduce the value of y_2 below its lower bound. Thus, we conducted another analysis shifting the lower bound of y_2 (i.e. upper bound of y_1) from 0.5 to 0.4. This time the analysis converged after 187 iterations in MATLAB, with a final cost $\tilde{J} = 173,833$ [kNs/m]. The values $y_1 = 0.2049$ and $y_2 = 0.4268$ were obtained, corresponding to the damping coefficients $\bar{c}_1 = 10,247$ [kNs/m] and $\bar{c}_2 = 21,342$ [kNs/m]. The modification of the boundaries of y_1 and y_2 was beneficial, since the algorithm converged to a better solution. As in the previous cases, the optimized \mathbf{x}_1 and \mathbf{x}_2 were not precisely binary and some minor rounding was performed. The original and rounded off optimized solutions are presented in Tab. 8.

k^{th} damper location	$\mathbf{x}_1(2k-1), \mathbf{x}_1(2k)$	$\mathbf{x}_2(2k-1), \mathbf{x}_2(2k)$	$\mathbf{x}_1^{rounded}(2k-1), \mathbf{x}_1^{rounded}(2k)$	$\mathbf{x}_2^{rounded}(2k-1), \mathbf{x}_2^{rounded}(2k)$
1	0, 0	N/A, N/A	0, 0	N/A, N/A
2	1, 0	0.9928, N/A	1, 0	1, N/A
3-9	0, 0	N/A, N/A	0, 0	N/A, N/A
10	1, 0	1, N/A	1, 0	1, N/A
11	1, 0	1, N/A	1, 0	1, N/A
12	1, 0	0, N/A	1, 0	0, N/A
13-16	0, 0	N/A, N/A	0, 0	N/A, N/A

Table 8: Optimal values of \mathbf{x}_1 and \mathbf{x}_2 achieved with the SLP in Ex. 4.2 considering simultaneously LA14 and LA16. The values of \mathbf{x}_2 not associated to an existing damper are irrelevant, and replaced with N/A (not applicable).

The optimized damper sizes and distribution in the potential locations considering the rounded optimized \mathbf{x}_1 and \mathbf{x}_2 are shown in Fig. 15. Fig. 16 shows the drift distribution for the optimized damper distribution. Only with the record LA16 the drift number 10 slightly exceeds the allowable value by 0.48% (0.0168 cm). Finally, the design solution respected the drift constraint for all the other records from the ensemble LA 10% in 50 years.

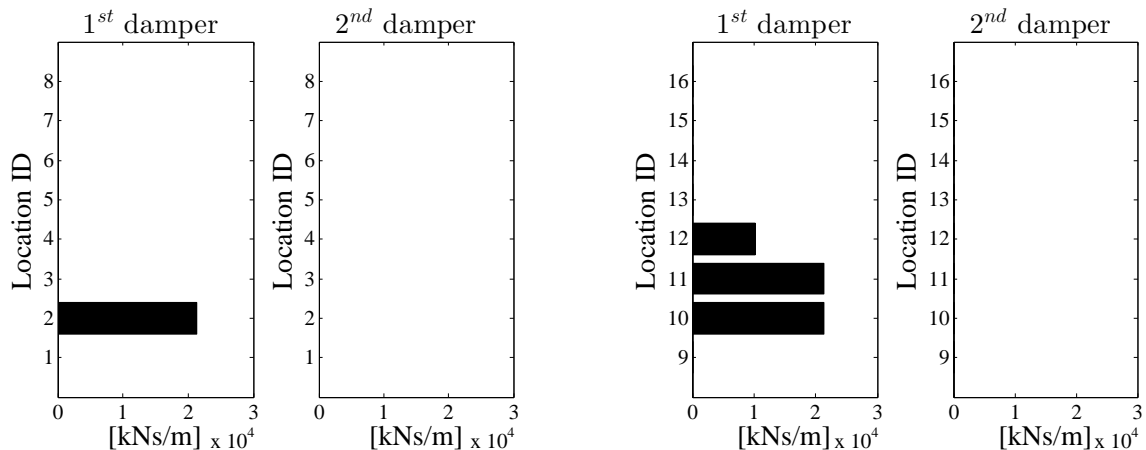


Figure 15: SLP solution. First and second damper for each location in Ex. 4.2 considering LA14 and LA16 simultaneously. The optimal distribution of damper resembles the one attained previously considering only LA16 (Fig. 11), but with the addition of a small damper in the 12th location.

In both Ex. 4.1 and Ex. 4.2 it can be seen that the SLP and the GA converged exactly to the same topological layout: Both procedures chose to allocate dampers in the same potential locations. At the same time, the two solutions differ slightly in the optimized damping coefficients for each size group of dampers and in the dampers' distribution within the chosen potential locations. Nevertheless, the

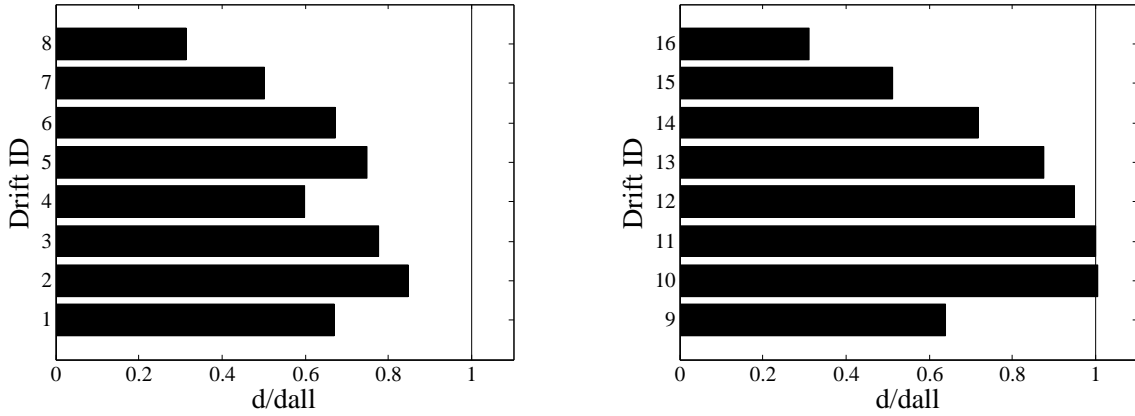


Figure 16: SLP solution. Drift distribution in Ex. 4.2 considering *LA14* and *LA16* simultaneously. For each drift is plotted the worst scenario. The drift number 10 exceeds the allowable value by the 0.48% due to the record *LA16*.

	\tilde{J} [kNs/m]	$\max(d_{c,max}/d_{all})$	\bar{c}_{d1} [kNs/m]	\bar{c}_{d2} [kNs/m]	Func. evaluations (gradient evaluations are included as function evaluations in the SLP)
SLP	173,833	1.0048 (0.48%)	10,247	21,342	$4 \cdot 187 \approx 10^{2.874}$

Table 9: Synthesis of the optimal solution achieved with the SLP in Ex. 4.2 considering *LA14* and *LA16* simultaneously.

final costs for the optimized solutions are very similar, demonstrating the abundance of local minima in proximity of the global optimum.

In the optimized solutions achieved by the SLP procedure, rather small constraint violations were observed. This can be due to: the approximations introduced in the *max* functions; the linearizations through which the problem is approximated; and some minor rounding applied on the optimized solutions. The main advantage of the SLP with respect to the GA is the considerably smaller computational effort required to achieve the optimized solution. In principle, the SLP requires two time history analyses for each iteration (for a single ground motion), while the GA needed 500 time history analyses for each generation (i.e. iteration) for all 20 different optimization processes performed.

The continuous approach suggested herein was also successful in adapting to higher costs of certain components. In Ex. 4.1 we performed an additional optimization while increasing the component $C_{prototype}$ from 10,000 [kNs/m] to 50,000 [kNs/m]. As expected, the SLP converged to an optimized solution characterized by a preference of only one size-group of dampers instead of a combination of the two size-groups available.

In Ex. 4.2 the optimized solution achieved with SLP did not fulfill the drift requirement for all the records in the ensemble. Thus an additional optimization has been performed considering simultaneously the records *LA14* and *LA16*. This led to a different damper distribution and sizing for which the computed drifts were smaller than the allowable limit for all the records of the ensemble.

5 Conclusions

In this paper we presented a novel, effective approach for achieving minimum-cost design of seismic retrofitting using viscous fluid dampers. A new realistic cost function is defined, enabling the optimal allocation and sizing of viscous dampers in frame structures for seismic applications. The new cost function mimics the cost of seismic retrofitting, taking into account its three main components: The work associated with the installation of a damper in a potential location of the frame and the architectural impediment caused by its presence; The direct manufacturing cost of the dampers; And the cost of prototype design and testing for each damper size. Constraints are imposed on peak inter-story drifts of

each story of each peripheral frame separately. These are assessed based on a given ensemble of realistic ground motions. The resulting optimization problem is highly nonconvex and nonlinear.

The optimization problem was first formulated in a mixed-integer framework, involving discrete and continuous variables. The mixed-integer problem was then solved using a Genetic Algorithm. The problem was then re-formulated using only continuous variables and applying interpolation techniques in order to attain discrete solutions. This problem was solved via a Sequential Linear Programming algorithm. Finally, the optimized designs of two case studies attained using the two approaches were presented and compared. The results revealed that the two algorithms converged to solutions with dampers at the same locations and with very similar damper sizes. At the same time, the Sequential Linear Programming algorithm converged to the optimized solution with a significantly smaller computational effort. This demonstrates that the proposed formulation and the first-order gradient-based algorithm can provide a very attractive framework for the practical design of seismic retrofitting using viscous dampers.

Acknowledgements

The authors are grateful to the anonymous reviewers for their helpful comments.

References

- Agrawal, A. K. and Yang, J. N. (1999). Optimal placement of passive dampers on seismic and wind-excited buildings using combinatorial optimization. *Journal of Intelligent Material Systems and Structures*, 10(12):997–1014. (page 2)
- Aguirre, J. J., Almazán, J. L., and Paul, C. J. (2013). Optimal control of linear and nonlinear asymmetric structures by means of passive energy dampers. *Earthquake Engineering & Structural Dynamics*, 42(3):377–395. (page 2)
- Almazán, J. L. and de la Llera, J. C. (2009). Torsional balance as new design criterion for asymmetric structures with energy dissipation devices. *Earthquake Engineering & Structural Dynamics*, 38(12):1421–1440. (page 2)
- Avishur, M. and Lavan, O. (2010). Seismic behavior of passively controlled frames under structural uncertainties. In *Structures Congress. Orlando, Florida*. (page 1)
- Bendsøe, M. P. (1989). Optimal shape design as a material distribution problem. *Structural Optimization*, 1(4):193–202. (page 8)
- Bendsøe, M. P. and Sigmund, O. (2003). *Topology Optimization: Theory, Methods and Applications*. Springer. (page 8)
- Bigdeli, K., Hare, W., Nutini, J., and Tesfamariam, S. (2015 (submitted)). Optimizing damper connectors for adjacent buildings. *Optimization and Engineering*, pages 1–19. (page 2)
- Charmpis, D. C., Komodromos, P., and Phocas, M. C. (2012). Optimized earthquake response of multi-storey buildings with seismic isolation at various elevations. *Earthquake Engineering & Structural Dynamics*, 41(15):2289–2310. (page 6)
- Cheney, E. W. and Goldstein, A. A. (1959). Newton’s method for convex programming and tchebycheff approximation. *Numerische Mathematik*, 1(1):253–268. (page 10)
- Christopoulos, C., Filiatrault, A., and Bertero, V. V. (2006). *Principles of Passive Supplemental Damping and Seismic Isolation*. IUSS Press. (page 1)
- Civicioglu, P. (2013). Backtracking search optimization algorithm for numerical optimization problems. *Applied Mathematics and Computation*, 219(15):8121–8144. (page 2)

- Constantinou, M. C., Soong, T. T., and Dargush, G. F. (1998). *Passive Energy Dissipation Systems for Structural Design and Retrofit*. Multidisciplinary Center for Earthquake Engineering Research Buffalo, New York. (page 1)
- Constantinou, M. C. and Symans, M. D. (1992). *Experimental and Analytical Investigation of Seismic Response of Structures with Supplemental Fluid Viscous Dampers*. National Center for Earthquake Engineering Research. (page 1)
- Dargush, G. F. and Sant, R. S. (2005). Evolutionary aseismic design and retrofit of structures with passive energy dissipation. *Earthquake Engineering & Structural Dynamics*, 34(13):1601–1626. (page 2)
- Eschenauer, H. A. and Olhoff, N. (2001). Topology optimization of continuum structures: A review*. *Applied Mechanics Reviews*, 54(4):331–390. (page 8)
- García, M., de la Llera, J. C., and Almazán, J. L. (2007). Torsional balance of plan asymmetric structures with viscoelastic dampers. *Engineering Structures*, 29(6):914–932. (page 2)
- Gidaris, I. and Taflanidis, A. A. (2014). Performance assessment and optimization of fluid viscous dampers through life-cycle cost criteria and comparison to alternative design approaches. *Bulletin of Earthquake Engineering*, pages 1–26. (page 3)
- Goel, R. K. (1998). Effects of supplemental viscous damping on seismic response of asymmetric-plan systems. *Earthquake Engineering & Structural Dynamics*, 27(2):125–141. (page 2)
- Goel, R. K. (2000). Seismic behaviour of asymmetric buildings with supplemental damping. *Earthquake Engineering & Structural Dynamics*, 29(4):461–480. (page 2)
- Guest, J. K., Prévost, J. H., and Belytschko, T. (2004). Achieving minimum length scale in topology optimization using nodal design variables and projection functions. *International Journal for Numerical Methods in Engineering*, 61(2):238–254. (page 8)
- Hvejsel, C. F. and Lund, E. (2011). Material interpolation schemes for unified topology and multi-material optimization. *Structural and Multidisciplinary Optimization*, 43(6):811–825. (page 8)
- Kanno, Y. (2013). Damper placement optimization in a shear building model with discrete design variables: a mixed-integer second-order cone programming approach. *Earthquake Engineering & Structural Dynamics*, 42(11):1657–1676. (page 2)
- Kelley, Jr, J. E. (1960). The cutting-plane method for solving convex programs. *Journal of the Society for Industrial & Applied Mathematics*, 8(4):703–712. (page 10)
- Kim, J. and Bang, S. (2002). Optimum distribution of added viscoelastic dampers for mitigation of torsional responses of plan-wise asymmetric structures. *Engineering Structures*, 24(10):1257–1269. (page 2)
- Lavan, O. (2012). On the efficiency of viscous dampers in reducing various seismic responses of wall structures. *Earthquake Engineering & Structural Dynamics*, 41(12):1673–1692. (page 1)
- Lavan, O. (2015 - accepted). Optimal design of viscous dampers and their supporting members for the seismic retrofitting of 3D irregular frame structures. *Journal of Structural Engineering, ASCE*, . (page 2)
- Lavan, O. and Amir, O. (2014). Simultaneous topology and sizing optimization of viscous dampers in seismic retrofitting of 3D irregular frame structures. *Earthquake Engineering & Structural Dynamics*, 43:1325–1342. (page 2, 8, 11)
- Lavan, O. and Dargush, G. F. (2009). Multi-objective evolutionary seismic design with passive energy dissipation systems. *Journal of Earthquake Engineering*, 13(6):758–790. (page 2)

- Lavan, O. and Levy, R. (2005). Optimal design of supplemental viscous dampers for irregular shear-frames in the presence of yielding. *Earthquake Engineering & Structural Dynamics*, 34(8):889–907. (page 10)
- Lavan, O. and Levy, R. (2006). Optimal peripheral drift control of 3D irregular framed structures using supplemental viscous dampers. *Journal of Earthquake Engineering*, 10(6):903–923. (page 2, 4, 6, 8, 11, 16)
- Lavan, O. and Levy, R. (2009). Simple iterative use of Lyapunov’s solution for the linear optimal seismic design of passive devices in framed buildings. *Journal of Earthquake Engineering*, 13(5):650–666. (page 2)
- Levy, R. and Lavan, O. (2006). Fully stressed design of passive controllers in framed structures for seismic loadings. *Structural and Multidisciplinary Optimization*, 32(6):485–498. (page 2)
- Lin, W. H. and Chopra, A. K. (2001). Understanding and predicting effects of supplemental viscous damping on seismic response of asymmetric one-storey systems. *Earthquake Engineering & Structural Dynamics*, 30(10):1475–1494. (page 2)
- Lin, W. H. and Chopra, A. K. (2003a). Asymmetric one-storey elastic systems with non-linear viscous and viscoelastic dampers: Earthquake response. *Earthquake Engineering & Structural Dynamics*, 32(4):555–577. (page 2)
- Lin, W. H. and Chopra, A. K. (2003b). Asymmetric one-storey elastic systems with non-linear viscous and viscoelastic dampers: Simplified analysis and supplemental damping system design. *Earthquake Engineering & Structural Dynamics*, 32(4):579–596. (page 2)
- Lopez Garcia, D. and Soong, T. T. (2002). Efficiency of a simple approach to damper allocation in MDOF structures. *Journal of Structural Control*, 9(1):19–30. (page 2)
- Miguel, L. F. F., Fadel Miguel, L. F., and Lopez, R. H. (2014). A firefly algorithm for the design of force and placement of friction dampers for control of man-induced vibrations in footbridges. *Optimization and Engineering*, pages 1–29. (page 2)
- Miguel, L. F. F., Miguel, L. F. F., and Lopez, R. H. (2015). Simultaneous optimization of force and placement of friction dampers under seismic loading. *Engineering Optimization*, (ahead-of-print):1–21. (page 2)
- National Information Service for Earthquake Engineering - University of California, Berkeley (N/A). 10 pairs of horizontal ground motions for Los Angeles with a probability of exceedence of 10% in 50 years. (page 11)
- Pollini, N., Lavan, O., and Amir, O. (2014). Towards realistic minimum-cost seismic retrofitting of 3D irregular frames using viscous dampers of a limited number of size groups. In *Proceedings of the Second European Conference on Earthquake Engineering and Seismology. Istanbul (Turkey)*. (page 3, 7)
- Shin, H. and Singh, M. (2014a). Minimum failure cost-based energy dissipation system designs for buildings in three seismic regions – Part I: Elements of failure cost analysis. *Engineering Structures*, 74:266–274. (page 3)
- Shin, H. and Singh, M. (2014b). Minimum failure cost-based energy dissipation system designs for buildings in three seismic regions – Part II: Application to viscous dampers. *Engineering Structures*, 74:275–282. (page 3)
- Singh, M. P. and Moreschi, L. M. (2001). Optimal seismic response control with dampers. *Earthquake engineering & structural dynamics*, 30(4):553–572. (page 2)
- Soong, T. T. and Dargush, G. F. (1997). *Passive Energy Dissipation Systems in Structural Engineering*. Wiley New York. (page 1)

- Stolpe, M. and Svanberg, K. (2001). An alternative interpolation scheme for minimum compliance topology optimization. *Structural and Multidisciplinary Optimization*, 22(2):116–124. (page 8)
- Takewaki, I. (2011). *Building Control with Passive Dampers: Optimal Performance-Based Design for Earthquakes*. John Wiley & Sons. (page 1)
- Takewaki, I., Yoshitomi, S., Uetani, K., and Tsuji, M. (1999). Non-monotonic optimal damper placement via steepest direction search. *Earthquake Engineering & Structural Dynamics*, 28(6):655–670. (page 2)
- Taylor, D. (2014). Personal communication. (page 5)
- Tso, W. K. and Yao, S. (1994). Seismic load distribution in buildings with eccentric setback. *Canadian Journal of Civil Engineering*, 21(1):50–62. (page 11)
- Wu, B., Ou, J. P., and Soong, T. T. (1997). Optimal placement of energy dissipation devices for three-dimensional structures. *Engineering Structures*, 19(2):113–125. (page 2)
- Yang, X.-S. (2008). *Nature-Inspired Metaheuristic Algorithms*. Luniver Press, United Kingdom, 1 edition. (page 2)
- Zhang, R. H. and Soong, T. T. (1992). Seismic design of viscoelastic dampers for structural applications. *Journal of Structural Engineering*, 118(5):1375–1392. (page 2)